UNIVERSIDADE DE BRASÍLIA
FACULDADE DE AGRONOMIA E MEDICINA VETERINÁRIA
PROGRAMA DE PÓS-GRADUAÇÃO EM AGRONOMIA

OBTAINING WATER STRESS INDEX FOR BEAN CROP USING THERMAL IMAGES

THATYANE KARY GRIGÓRIO DE SOUZA

MASTER`S THESIS IN AGRONOMY

BRASÍLIA/DF
JULY/2022

UNIVERSIDADE DE BRASÍLIA
FACULDADE DE AGRONOMIA E MEDICINA VETERINÁRIA
PROGRAMA DE PÓS-GRADUAÇÃO EM AGRONOMIA

OBTAINING WATER STRESS INDEX FOR BEAN CROP USING THERMAL IMAGES

THATYANE KARY GRIGÓRIO DE SOUZA

ADVISOR: DR. JOÃO JOSÉ DA SILVA JÚNIOR

MASTER`S THESIS IN AGRONOMY

PUBLICATION: NÚMERO DA DISSERTAÇÃO/2022

BRASÍLIA/DF
JULY/2022

UNIVERSIDADE DE BRASÍLIA

FACULDADE DE AGRONOMIA E MEDICINA VETERINÁRIA

PROGRAMA DE PÓS-GRADUAÇÃO EM AGRONOMIA

OBTAINING WATER STRESS INDEX FOR BEAN CROP USING THERMAL IMAGES

THATYANE KARY GRIGÓRIO DE SOUZA

DISSERTAÇÃO DE MESTRADO SUBMETIDA AO PROGRAMA DE PÓS-GRADUAÇÃO EM AGRONOMIA, COMO PARTE DOS REQUISITOS NECESSÁRIOS À OBTENÇÃO DO GRAU DE MESTRE EM AGRONOMIA.

APROVADA POR:

_____

JOÃO JOSÉ DA SILVA JÚNIOR, Dr. - FAV/Universidade de Brasília

_____

REJANE ENNES CICERELLI, Dr. PPGGAG/PTARH/Universidade de Brasília

_____

BRUNO MONTOANI SILVA, Dr. DCS – Universidade Federal de Lavras

BRASÍLIA/DF, August 10th of 2022

MODELO DE FICHA CATALOGRÁFICA

Thatyane Kary Grigório de Souza.

Obtaining water stress index for bean crop using thermal images

70p.: il.

Dissertação (Mestrado em Agronomia) - Universidade de Brasília / Faculdade de Agronomia e Medicina Veterinária, 2021.

1. Irrigação de precisão 2. Sensoriamento Remoto 3. Imagens termais 4. Estresse hídrico
I. Silva Junior, J.J. II Drº

REFERÊNCIA BIBLIOGRÁFICA / BIBLIOGRAPHY REFERENCE

SOUZA, T. K. G. Obtaining water stress index for bean crop using thermal images: Faculdade de Agronomia e Medicina Veterinária, Universidade de Brasília, 2022, 70 páginas. (Dissertação de Mestrado em Agronomia).

CESSÃO DE DIREITOS

Nome do Autor: Thatyane Kary Grigório de Souza

Título da Dissertação de Mestrado: Obtaining water stress index for bean crop using thermal images.

Grau: Mestrado Ano: 2022

_____

THATYANE KARY GRIGÓRIO DE SOUZA

email: thatyanekary@hotmail.com

ACKNOWLEDGMENTS

I would like to thank God, who I truly believe and has given me strength to go through my days, and given me wisdom to finish this.

I would like to thank my mom, who has loved me unconditionally – I love you forever and forever will never be enough. I thank you for support and love.

I would like to thank my family for the love and encouragement. Vó e vô, I love you, you are the people who the most inspire me in this world.

I would like to thank professor João José for patient, support and contributions during my master's.

I would like to thank professor Nicolas and Brigitte for the support and contributions on this work.

I would like to thank my colleagues who helped me to conduct the experiment, Andressa and João, and the collaborators from the Biology station at UnB, who helped me. Also, my Canada lab mate, Ahmed.

I would like to thank my friends, flatmates and colleagues who I have met during my master's for the time we spent together chilling, laughing and for the days overcoming stress, anxiety and sadness.

I would like to thank everyone who has support me and encourage me to achieve my dreams during this journey.

I would like to thank the institutions that sponsored this project: CAPES, CNPq (chamada MCTIC/CNPq Nº 28/2018 Processo: 423744/2018-6), and ELAP.

I feel very grateful for everyone and every little single thing during my master's.

RESUMO

Imagens baseadas em sensoriamento remoto têm se mostrado uma boa ferramenta para avaliar o estresse hídrico em plantas. O feijão é uma das culturas mais cultivadas no Brasil, considerando isso, o objetivo deste trabalho foi utilizar imagens térmicas da temperatura do dossel para melhorar a eficiência hídrica da cultura e monitorar o estresse hídrico, nos potenciais de água no solo para o Latossolo Vermelho e o Latossolo Amarelo (-10, -20, -25, -30 e -40 kPa) e o Neossolo Regolítico (-5, -10, -15, -20 e -25 kPa). O potencial matricial do solo (SMP) e o potencial hídrico foliar (LWP) foram medidos in situ, as imagens térmicas do dossel do feijoeiro foram capturadas, usando uma câmera térmica, para calcular o CWSI (Crop Water Stress Index). Avaliou-se a relação entre esses indicadores de estresse, para os estádios de crescimento do feijoeiro, por meio de equações de regressão. O modelo de predição do SMP obtida em ambiente controlado foi aplicada em uma área de pivô central cultivado com feijão, utilizando uma câmera térmica acoplada a um veículo aéreo não tripulado (VANT) para avaliar o estresse hídrico. Adicionalmente, mapas de CWSI e potencial matricial do solo foram criados para avaliar a variabilidade espacial dos níveis de estresse e a disponibilidade de água nas plantas. A relação entre CWSI e SMP para o estágio V4 foi robusta (R^2=0.95) e significativa (p-valor < 0.05) para o Neossolo Regolítico. Nos estádios R5_R6, para o Latossolo Vermelho-Amarelo, a relação foi alta e significativa (R^2=0.86; p-valor < 0.05). No estádio R7, o Latossolo Vermelho apresentou coeficiente de determinação robusto (R^2=0.8265) e a regressão foi significativa (P<0.032), o Latossolo Vermelho-Amarelo (R^2=0.9795; p-valor < 0.05). Enquanto no estádio R8, a correlação foi elevada e significativa para o Latossolo Vermelho-Amarelo (R^2=0.9596; p-valor < 0.05), e para o Neossolo Regolítico (R^2=0.95) e (p-valor < 0.05). As relações entre CWSI e LWP foram altas para o Latossolo Vermelho (R^2=0.87) e Neossolo Regolítico (R^2=0.92), enquanto que para o Latossolo Vermelho-Amarelo a regressão foi fraca, mas não significativa (p-valor >0.05) para todos os solos tipos neste estudo. O modelo de regressão no estágio R8 (R^2=0.96) obteve melhor ajuste do SMP em resposta ao CWSI no Neossolo Regolítico. Dados obtidos em campo e no ambiente controlado foram usados para analisar a performance desse modelo (R^2=0.85, RMSE=3.08, MAE=2.34). O modelo foi aplicado para desenvolver os mapas de CWSI e mapas de potencial matricial do solo, que mostraram a variabilidade dos níveis hídricos e de estresse nas plantas. Esses resultados evidenciam a potencial uso de imagens térmicas obtidas por VANTs para manejo de irrigação de precisão.

Palavras-chave: temperatura do dossel; déficit hídrico; agricultura de precisão.

ABSTRACT

Remote sensing-based images has been showing as a good tool to assess water stress in plants. Bean is one of the most crops cultivated in Brazil, considering that, the aim of this paper was to use thermal images of canopy temperature to improve crop water efficiency and monitor water stress. The experiment was conducted in a controlled environment applying different irrigations depths based on soil matric potential for the Red Latosol and the Yellow Latosol (10, -20, -25, -30 and -40 kPa) and the Regolithic Neosol (-5, -10, -15, -20 and -25 kPa). Soil matric potential (SMP) and leaf water potential (LWP) were measured, and thermal images were taken from canopy using a thermal camera to compute the CWSI (Crop Water Stress Index). We evaluated the relationship among these stress indicators, for growth stages of bean, through regression equations. Prediction model obtained in controlled conditions was applied at a center-pivot irrigation field cultivated with bean, using thermal images by an unmanned aerial vehicle (UAV) to asses water stress. Additionally, maps of CWSI and soil matric potential were created to evaluate the spatial variability of stress levels and the availability of water in plants. The relationship between CWSI and SMP at V4 stage was robust and significant (R^2=0.95; p-value < 0.05) for the Regolithic Neosol. At stages R5_R6, for the Red-Yellow Latosol the relationship was strong and significant (R^2=0.86; p-value < 0.05). At stages R7 the relationship was significant and presented a robust coefficient of determination for the Red Latosol (R^2=0,8265; p-value<0.032) and for the Red-Yellow Latosol (R^2=0.9795; p-value < 0.05). At R8 stages, the regressions were significant and strong for the Yellow Latosol R^2=0.9596; p-value < 0.05) and for the Regolithic Neosol (R^2=0.96). The relationship between CWSI and LWP were strong for the Red Latosol (R^2=0.87) and Regolithic Neosol (R^2=0.92), whereas for the Yellow-Red Latosol the regression was weak, but not significant (p-value >0.05) for all soil types in this study. The regression model at R8 stage (R^2=0.96) obtained the best performance of CWSI in predict the SMP for the Regolithic Neosol. Data obtained in the field and in the controlled environment were used to analyze the performance of this model, results indicated a good agreement between predicted and measured SMP (R^2=0.85, RMSE=3.08, MAE=2.34). The model was able to mapping the soil matric potential maps and CWSI maps showed the variability of water and stress levels in plants. These results highlight the potential of thermal images obtained from UAV for precision irrigation management.

Key-words: canopy temperature; water deficit; precision irrigation

TABLE OF CONTENTS

LIST OF FIGURES

LIST OF TABLES

1 INTRODUCTION

Water is an essential resource for plant growth. The limitation of water for crop growth in the environment is the main reason for irrigation. In this respect, is it necessary to understand how water is released from the soil and uptake by plants (TAIZ: ZEIG, 2015), additionally, it is necessary to take in consideration the current availability of water and climate change scenarios, which plays a major influence in the dynamic of water management, especially in agricultural fields. The agricultural field is heterogeneous, identifying the spatial variability of soil, crops, soil cover, and plant canopy is relevant for efficient irrigation management (COUVREUR et al., 2016). According to Gonzalez-Dugo et al., (2021), a wide of irrigation techniques can be used to optimize water use efficiency while increasing crop yield, particularly irrigation strategies such as deficit irrigation, reducing water losses and precision irrigation. The characterization of spatial variability of cultivation areas and crop water requirements are prerequisites for precision irrigation. Precision irrigation is a key component to improve water efficiency in agriculture systems, it can be applied variable rate irrigation and identify areas more susceptible to water stress in the field, aiming high crop productivity.

Irrigation programs need to be developed based on crop, climate and soil indices. Thus, applying water supply rates and amounts based on plant requirements and local demand, by identify the areas most sensitive to water stress within a field. To assess the state of water in the plants, new methods have been studied over the years. Plant indices such as leaf and stem water potential, and canopy temperature are used to determine the time of irrigation. In particular, some studies have shown the potential of using canopy temperature to monitor the water status of plants. Compared to traditional methods, this method yields a reliable index for irrigation management and has the advantage of being quick, very operational and non-destructive (KHORSAND et al., 2019). According to Bellvert et al. (2016), measuring canopy temperature is a practical and effective alternative method for measuring leaf water potential. Infrared thermometers have been largely used to measure canopy temperature. However, thermal imaging of crops is now widely considered to detect water stress in crops and for irrigation management purposes (Costa at al., 2018; Ramirez at al., 2015).

González-Dugo et al. (2013) suggest that temperature-based crop water stress indices are inversely related to transpiration rate and stomatal conductance. Such indices have been successfully associated with indicators of plant water status, such as leaf water potential. According to Maes; Steppe (2012), at the onset of water stress, the stomata close and

transpiration rates and evapotranspiration cooling are reduced. In turn, leaf temperature increases, making it a proxy for these different leaf water-related processes.

For a reliable water stress index for irrigation management, the index must be calibrated against a specific crop. Crop Water Stress Index (CWSI), for example, in an index that is determined based on canopy temperature (CHASTAIN et al., 2016). Once calibrated, it is a reliable indicator of soil water availability. The calibration process should include an experiment in a controlled environment to protect the crop plants against external agents, mainly meteorological agents. In addition, under these controlled conditions, light, nutrient and water limitations can be eliminated.

Among all the bean species cultivated in Brazil, *Phaseolus vulgaris*, also known as common bean and French bean, is the most popular. Beans are quite sensitive to water stress and when water deficits occur in critical periods of development, they can compromise the development of the root system and cause a significant reduction in productivity. For the common bean, water stress in the phases of flowering and pod filling reduces the number of pods and seeds per plant as well as seed size, consequently, significantly reduces yields (MATHOBO et al. 2017; GALVÃO at al. 2019). The estimation of a fast and reliable water stress index for the common bean will allow for a more precise and variable management of irrigation in Brazil.

1.1 General objective

Considering the above, it is necessary to optimize water use and irrigation management in bean crops in Brazil. In this thesis, we focus on the use of infrared thermal imaging using unmanned aerial vehicles technology which provides the possibility of mapping the spatial variability of crop temperature and in turn, the estimation of water status of crops.

1.2 Specific Objectives

- Compare Crop Water Stress Index obtained from high resolution thermal images of bean to the leaf water potential in function of different soil matric potentials and types of soil.
- Obtain the relationship between leaf water potential of bean and the soil matric potential.
- Obtain the relationship between Crop Water Stress Index derived from high resolution thermal images of bean to leaf water potential in function of different soil matric potentials.

2 HYPOTESES

- Correlate the water stress index of the bean crop, obtained through canopy temperature, with the leaf water potential and soil matric potential.
- Determine the irrigation depth of bean crop through the direct correlation between Crop Water Stress Index, obtained from canopy temperature, and soil matric potential.

3 LITERATURE REVIEW

3.1 Precision irrigation

According to Plaščak et al., (2021), the first researches involving precision irrigation was in the decade of 90 in the United States. The purpose was to change mobile irrigation systems which are using in large areas and requires a large amount of water, considering the field heterogeneity. Thus, based on that yield can be increase if the plant receives adequate amount of water it requires. The use of precision irrigation was unanimous to determine properly depth of water application, according to the crops water requirements. Precision irrigation can be defined as the use of techniques and strategies that aims optimize the efficiency of water applied for crop to maximize yield, based on the crops water requirements. Therefore, this system aims more precisely the application of water in agricultural field, considering the heterogeneity of soil, spatial and temporal variability of water in plants, aiming to provide adequate quantity of water requires by crops. Additionally, precision irrigation optimizes the nutrient use (SIKKA, 2018).

First studies showed that this type of system was more suitable for farmers with a large production due to the cost and complexity of them. Later in the 2000's researches focused on the application for the application of spatially different irrigation rates (AL-KARADSHEH et al., 2002). Over the years the number of researches regarding precision irrigation increased, Peters and Evett, (2004) used the temperature-time threshold (TTT) index to manage the irrigation in a center pivot by monitoring the canopy temperature, as an alternative to the traditional methods of soil water irrigation. They also concluded that this method was accessible for small farmers. O'Shaughnessy et al., (2008) investigated the use of infrared thermometers to measure crop canopy temperature for irrigation scheduling.

Precision irrigation requires more accurately in collecting crop and soil data which reflects the soil and crop condition in the field, for that, devices are used to identify and quantify

these data to apply precision irrigation. The monitoring of spatial variability can be continuously, in situ or remotely. Sensors to perform the measurements in the field can be classified as contact and remote sensors. Remote sensing methods are more indicate for application in precision irrigation, once they are more suitable for compute spatial variation by using high resolution images. High resolution remote sensing systems are able to provide information regarding water stress condition in plants (PLAŠČAK et al., 2021).

Sensors are commonly coupled on satellites, aerial, and ground-based platforms. When compare to the aerial platforms such as UAVs, in general, satellites can achieve lower spatial resolution (SISHODIA et al., 2020). The acquisition of commercial satellites high spatial resolution images is costly, therefore, the UAVs can be an alternative method low-cost. The initial investment of UAVs is high, considering equipment, data processing and software, limiting the acquisition by farmers or for commercial scale, the development and investment of sensors with low-cost may become this technology more accessible for farmers (EHSANI at al., 2013; HONRADO et al., 2017).

Some sensors largely used for precision irrigation application in the field are multispectral sensors and thermal infrared sensors. Data collected from sensors provides information for the detection of plant stress. A wide range of indices is available to assessing water status in the soil and in the plants. The normalized difference vegetation index (NDVI) can be obtained from multispectral sensors, this index can detect water stress and determine soil moisture for crops. On the other hand, thermal sensors data are used to calculate indices based on canopy temperature, the most common is crop water stress index (CWSI). Additionally, thermal information can be used to create maps of water variability in the agricultural field such as soil matric potential, as well as, thermal temperature and crop water stress maps (SISHODIA et al., 2020; PLAŠČAK et al., 2021).

3.2 Plant-based crop management techniques

3.2.1 Infrared thermometry

Infrared thermograph has been used since 1960 to measure the temperature of vegetable surfaces, but it became more used in in 1970 when small and portable infrared thermometers were developed. The initial use of the infrared sensors was to identify water stress in plants under different irrigation depths (FUCHS; TANNER 1966). According to Khanal at al., (2017)

this technology became more popular when the crop water stress index (CWSI) was developed, which aimed to indicate the need of water in irrigation systems.

The water stress in plants can be detected in early stages through images techniques in a fast and non-destructive way, thermography and multispectral images are the newest and the most developed technique. This technology allows to measure the canopy temperature on one leaf or a set of leaves, small and vast areas. Leaves of plants under water stress tends to increase the leaf temperature and more infrared radiation will be emitted (ZHUANG et al., 2018).

The disadvantage of the infrared digital camera is the high investment to its acquisition. Otherwise, the advantages are to measure in real time, the equipment is portable, slight, and easy to manage; it has a good precision and sensitivity in its sensors, in addition, the high capacity to store data. The camera software allows the measurement of the temperature in any area of the thermogram (GODYN et al., 2013).

The cameras have the ability to perform more accurately measurement of the leaf temperature, as they provide instantaneous temperature of the entire canopy. Thermal imaging cameras show the difference between well-watered plants and no-watered plants, as well as different irrigations depts (ZARCO-TEJADA et al., 2012). To identify water stress in plants, some studies have been conducted using infrared thermograph and canopy temperature, i,e., COHEN et al., 2017; BELLVERT et al., 2016; GONZÁLEZ-DUGO et al., 2013, vines (LEINONEN; JONES, 2004) and cotton (ALCHANATIS et al., 2010; PADHI et al., 2012).

Ballester et al. (2013) obtained the leaf temperature using a thermal camera to assess water stress in citrus and persimmon trees, the results showed the capability of thermal images to detect stress persimmon trees were better when compared to citrus. Romano et al. (2011) used thermal images to select genotypes of maize for drought tolerance, they found that the canopy difference is more perceptive in genotypes under stress compared to genotypes in a unstressed condition, in addition to thermal images were more accurate in detect water stress in the grain filling stage. Rud et al., (2014) obtained the crop water stress index based on canopy temperature in potato using thermal imaging, their results showed that this technique is an effective tool to detect water stress.

3.2.2 Canopy temperature

Canopy temperature and stomatal conductance are methods to schedule irrigation, due to their capacity to monitor the water stress in plants (KHANAL at al., 2017). According to ĆOSIĆ et al., (2018), canopy temperature is a fundamental tool to assess the drought stress in

plants, being useful to schedule the moment of irrigating, considering the relations between leaf cooling and evapotranspiration. The canopy temperature is able to detect water stress in plants in field or controlled conditions.

The roots are responsible for water uptake from the soil, the water goes to the entire plant, through xylem tissues until reaches the epidermic of leaf, where the stomata and cuticles are located, they are responsible to evaporate the water, process known as evaporative cooling. Plants absorb solar radiation, which causes the increase of leaf temperature, this is controlled by the evapotranspiration of plants, where the heat accumulated in the leaves needs to be dissipated. Foliar transpiration is a common process used by the plants to dissipated heat thought water vapor. (ĆOSIĆ et al., 2018; COSTA et al., 2013).

Stomata are important leaf structures to the evapotranspiration process, cooling the leaf, they are related to the availability of water in the soil, and to meteorological conditions at a given time (ELSAYED et al, 2017). A plant under a stress condition will close partially or totally the stomata, to avoid the loss of water. Thus, increasing the leaf temperature, because the transpiration process is reduced when compared to a non-stressed plant (IHUOMA; MADRAMOOTOO, 2017; BANERJEE et al., 2020).

Infrared thermometers are the oldest method to measure the canopy temperature, but the infrared thermal camera has been used the latest technique to evaluate the water status in plants, specially, the measurements of canopy temperature in plants under stress conditions. This statement is based on that the difference between the canopy temperature and air temperature (Tc - Ta) increases according to low availability of water in the soil and in the plants, whereas the evapotranspiration is reduced (FUCHS; TANNER 1966).

Ćosić et al. (2018), who evaluated the effect of kaolin on leaf temperature for tomato and pepper. For all the treatments applied, the leaf temperature increased due to the decreasing of irrigation depths, it had a significant effect in a water stress condition. In tomatoes was observed that the well irrigated plants showed the lowest canopy temperature, not affecting the transpiration rate of the plants, considering the adequate supply of water in the soil and uptake by the plants.

3.2.3 Irrigation management indices using thermometry

Indices has been developed to monitor and measure the water stress using infrared thermometry. The canopy temperature is used as a main parameter for evaluation in all the

indices (DEJONGE et al., 2015). The efficiency and limitations have been defined as parameters which one fits better to compute and monitor the water deficit in plants.

According to Costa et al., (2018), The Stress Degree Day (SDD) was developed by Jackson et al. (1977), to identify water stress in plants. The SDD is defined as the difference between a canopy temperature and air temperature for a given period of time. Plants are considered non-stressed when the canopy temperature is lower than air temperature. Otherwise, plants are considered under stress, when the canopy temperature is higher than air temperature. The disadvantage of the SDD is not including the influence of vapor pressure deficit (VPD), solar radiation, and wind speed on plants (DEJONGE et al., 2015).

Temperature Stress Day (TSD) is computed as the difference between temperature of a stressed canopy and temperature of an unstressed canopy of the same crop species. The main disadvantage of this method is that it does not take into consideration that the climate conditions may affect the index, i.e, relative humidity (DEJONGE et al., 2015).

According to Taghvaeian et al., (2014), the Degrees Above Non-Stressed Canopy (DANS) requires the difference between stressed canopy temperature (actual temperature of the canopy of crop of interest) and non-stressed canopy temperature, and the DANS was an effective index to monitor water stress in sunflower crop.

Temperature-time threshold (TTT) is a Biologically-Identified Optimal Temperature Interactive Console (BIOTIC) method for irrigation management, which has been used for crop as soybean, cotton, maize, and sorghum. It consists of a crop threshold temperature and daily time the canopy temperature is above this threshold temperature. According to this method, the plants should be irrigated when the canopy temperature reaches the threshold temperature (TAGHVAEIAN et al., 2014; DEJONGE et al., 2015). According to Dejonge et al., (2015), two disadvantages can be found, first, the method do not include the degree of severity above the threshold, second, the need of irrigation do not respond to air temperature influences in the canopy temperature.

3.2.4 Crop water stress index (CWSI)

The Crop Water Stress Index (CWSI) was created by Jackson et al., (1981), which is the most popular index used to identify and monitor water stress in plants based on canopy temperature (ĆOSIĆ et al., 2018). This is based on the fact that the transpiration process in plats is responsible for cooling the leaf, once the soil water content available for plants is decreasing,

the transpiration and stomata conductance are reduced, then, the leaf temperature increases (IHUOMA; MADRAMOOTOO, 2017).

According to Khanal at al., (2017), the CWSI is obtained from the difference between the canopy temperature and air temperature (Tc-Ta), considering the evaporative demand of plants. For that was developed the lower baseline, which is when canopy transpiration rate is at its potential rate and the upper baseline, whereas, is when the transpiration rate is low or a non-transpire canopy. Thus, the real transpiration rate of a crop is determined using (Tc-Ta), vapor pressure deficit, atmospheric conditions, and crop characteristics to quantify the waster stress in plants, through the leaf (SEZEN et al., 2014; RAMÍREZ et al., 2015).

There are the empirical (Idso et al., 1982) and the theorical method (Jackson at al., 1981, 1988) to stablish the upper and lower baselines temperature for the CWSI. The empirical methods require only the air temperature, relative humidity and canopy temperature. Then, (Tc-Ta) is a linear regression against the vapor pressure deficit (VPD). The CWSI computed from this method, the relationship is considered as a lower baseline, defined as well as non-stressed baseline (NWSB). The CWSI is obtained from the linear relationship between (Tc-Ta) against vapor pressure gradient, known as the non-transpire baseline. The theorical CWSI requires more data and takes account of the energy balance of the crop.

Plant-based indices for irrigation scheduling need a threshold limit where the amount and the irrigation time is needed. Monitoring the water status regularly in plants and in the soil is important to not exceed the critical values (Ballester et al., 2013). The Crop Water Stress Index ranges from 0 to 1. When the canopy transpiration is at its potential rate, the CWSI tends to 0, mainly after irrigation. Otherwise, the availability of water in the soil or in the plant is decreasing, the CWSI will increase to 1 (O'SHAUGHNESSY et al., 2012). The higher is the CWSI value, the higher is the water stress.

According to Chen at al., (2010), o CWSI can be characterized as an index to schedule irrigation, may predict when water is required by plants, but it does not provide the amount or irrigation required by plants. The CWSI should be used in concomitance to other methods to provide water, such as soil moisture and leaf water potential measurements. Thus, the CWSI is an additional approach and is a consistent tool for decision making and irrigation management.

Silva et al., (2018) evaluated the water stress in tomatoes for different irrigation depths, the results showed that CWSI is effective for scheduling irrigation time. The highest CWSI value were found in the treatment with lowest soil water content, and the lower CWSI was significant in reducing yield. Xu et al., (2016), found that water stress was detected effectively using the canopy temperature obtained from thermal digital cameras. Besides that, the CWSI,

the stomatal conductance and the transpiration rate reduced at high CWSI values. Chastain et al., (2016) suggested that a calibrated CWSI based on canopy temperature is a good index for indicating soil water content. According to Alghory; Yazar (2019) the CWSI was effective to monitor the water potential for wheat crop, the lower content of water in the soil, the higher the canopy temperature.

3.3 Leaf Water Potential

According to Gadner (1960), the movement of water in soil-plant-atmospheric system occurs due water potential difference, from soil to the root, and from the xylem to leaves, the water flows from zones where the potential energy is higher i.e., in the soil, to zones where the potential energy is lower, i.e., the atmosphere. Thus, when the soil water content is decreasing, also the water potential in the soil and leaf are reducing. This creates a water deficit in the leaf, its mechanisms are to close the stomata, because the guard cells loss the turgor pressure (SLATYER, 1967), which is affected by leaf water potential, air temperature, CO_2 concentration, and light (KETELLAPER, 1963). According to Jarvis (1979), leaf water potential (LWP) is the energy in terms of amount of water at the liquid phase in the leaf. Leaf water potential allows to quantify the amount of water and the energy status in the plants (ELSAYED et al., 2011).

To understand the changes of plants physiological relations associated to leaf water potential is fundamental to monitor the drought tolerance of species and genotypes under water deficit conditions, once the loss of water by stomata is closely related to low water potential. As an alternative to drought tolerance is the maintenance of availability of water for plants under water stress (DJEKOUN; PLANCHON, 1991). According to Ding et al., (2014) the leaf water potential is an indicator of water stress in plants, and it can be used for irrigation scheduling and to understand plant-water relations.

The pressure chamber of Scholander is a traditional, reliable and widely method to measure the water pressure of plant tissues, i.e., leaf water potential in plants (DING eta al., 2014). The method is known as pressure bomb, consists in collect a leaf from the plant, and place the entire sample inside a cylinder, only the petiole remains outside. The chamber has a rubber cover to seal the sample inside the cylinder.

According to Furlan (2017), on the extremity of petiole is made a transversal cut. Then, chamber is submitted a pressure until the it causes exudation of water in the leaf, when

exudation is done, the supply of gas (inert gas, i.e., nitrogen) is interrupted, and the pressure reading is computed by a monometer. The reading corresponds to the water potential in the leaf.

Argyrokastritis et al., (2015) found that the LWP was affected by the irrigation's depths applied for 2 cultivars of cotton, the LWP was higher in the treatments with full irrigation when compared to the treatments with deficit irrigation. According to Chastain et al., (2016), the leaf water potential was able to determine the irrigation time for cotton. Bellvert et al., (2014) found a strong relationship between the leaf water potential (measured at a noon) and the CWSI.

The results of Jiang et al. (2013) showed that low leaf water potential is associated to low soil water content. Ali et al. (2014) found for crop growth stages a significant linear regression between the leaf water potential and the irrigation depths. The leaf water potential decreased as the irrigation depth decreased from 100% of evapotranspiration (ETo) to 60% of Eto. Alghory; Yazar (2019 found for wheat crop that the treatment that received irrigation, the well irrigated treatment (ETo 100%) showed a higher leaf water potential when compared to the less irrigated plants. Results were similar for the rainfall treatment, except at the flowering stage. Also, Kirnak et al. (2019) found a significant correlation between CWSI and leaf water potential for pumpkin under different irrigation depths.

3.4 Soil matric potential and water retention curves

The status of the water in the soil is characterized by the content of water and energy related to the force that water is held by the soil matrix (soil particles and pore space). The status of water in the soil plays a role in the plant growth, in the soil water-movement, temperature, light, chemical transport, groundwater recharge, crop water stress, and evapotranspiration (IRMAK, 2019). The water movement occurs inside the soil profile, between soil and roots of the plants, and between soil and atmosphere. The movement of water depends on the energy potential gradient (BILSKIE, 2001), soil matric potential is an important tool for irrigation scheduling.

According to Bilskie (2001), there are some fundamentals forces responsible to hold water in the soil, they are known as gravitational, matric and osmotic potential. The matrix of soil has capillaries and adsorptive (adhesion of water to solid soil surfaces) forces that determine the soil matric potential. The strength of them depends on the soil texture and physical-chemical properties of the solid material in the soil. Therefore, soil matric potential describes the energy state of water in the soil relative to the reference potential zero (pure water), it is important to understand the water flow.

According to Marshall (1959), the soil matric potential (SMP) is the tension level at which the water is held by the soil particles. It represents the energy to be applied for water to be extracted from the soil particles. The soil matric potential tends to 0 where there is no external force acting on water molecules, when the soil is saturated, to negative values, when the water content of the soil decreases.

One of the methods to measure the soil matric potential in situ is using tensiometers, the most common method (CONTRERAS et al., 2017). Tensiometers are equipment which gives the tension where the water is held by soil solid particles. The water retention curve describes relationship between the soil matric potential and soil water content of a given soil. In clay soils, where has fine texture, at a given potential, more water is held by the soil particles. Soil with coarse texture, i.e. sandy soils, they have more largely pores that hold less water (BILSKIE, 2001). Using the soil water retention curve and soil matric potential is possible to know soil water content, in turn, the amount of water to be applied in the soil. It represents the water available to plants (BASSOI; NASCIMENTO, 2012).

Quiloango-Chimarro et al., (2021) used tensiometer to monitor the soil matric potential and to scheduling irrigation to determine yield in beans under the water stress. Campos et al., (2021) also used the soil matric and soil water retention curve to manage irrigation in beans. Costa et al., (2018), Wang et al., (2007), Nascimento et al., (2022), Khatar at al., (2017), Domingues et al., (2018) used the tensiometer to monitor the availability of water in the soil. Contreras at al., (2018) and Kumar at al., (2019) scheduled different irrigations strategies based on the soil matric potential to evaluate the soil water content. Wang et al., (2007) found that the treatments with the highest soil matric potential the highest were the content of water in the soil when compared with those treatments under lower soil matric potential.

4 MATERIAL AND METHODS

4.1 Study Location

The experiment was conducted in a controlled environment located at the Experimental Biological Station, on Darcy Ribeiro Campus (DF) of the University of Brasília (15°44'S; 47°52'W). According to Köppen-Geiger classification, the climate of the region, is tropical (Aw), with a dry season in winter. Average annual precipitation is 1360 mm, and average annual maximum and minimum temperatures are 26.7°C and 16.1°C, respectively (CARDOSO et al., 2014).

The controlled environment consisted of a greenhouse (30 m × 13 m) equipped with an evaporative air-cooling system composed of an expanded clay panel with a motor-pump used to hold water to the upper part of the panel. In addition, eight exhaust fans with an individual removal capacity of 450 m^3 air min^{-1} were installed on the opposite side of the expanded clay panel for optimal removal of moisture in the interior air. The activation control of the cooling system is based on the interior air temperature, adjusted by a thermostat at 27 °C installed in the central part of the greenhouse at a height of 2 m from the ground (PEREIRA, 2021).

The greenhouse rooftop is made of a transparent plastic cover (diffuser film) and black screen cover, whereas the sides are made of asbestos tiles. For the specific experiment, the black screen was removed to reduce shading on the plants and because the bean crop requires a good amount of light interception (Silva et al., 2020).

4.2 Experimental design

The experiment was a randomized complete block design (RCBD), with four replications of five soil matric potential levels and three soil types. These treatments are detailed in sections below. We had 120 pots, but a total of 60 were used for measurements.

The pots were placed in the greenhouse along ten rows. Rows were 1.0 m apart, whereas pots were 0.4 m apart along the rows. Each row consisted of twelve pots, for a total of one hundred and twenty pots. Pots were placed on 9-hole bricks to avoid direct contact with flooring, thus minimizing the effects of disease transmission (the site has a history of transmission of various fungal diseases).

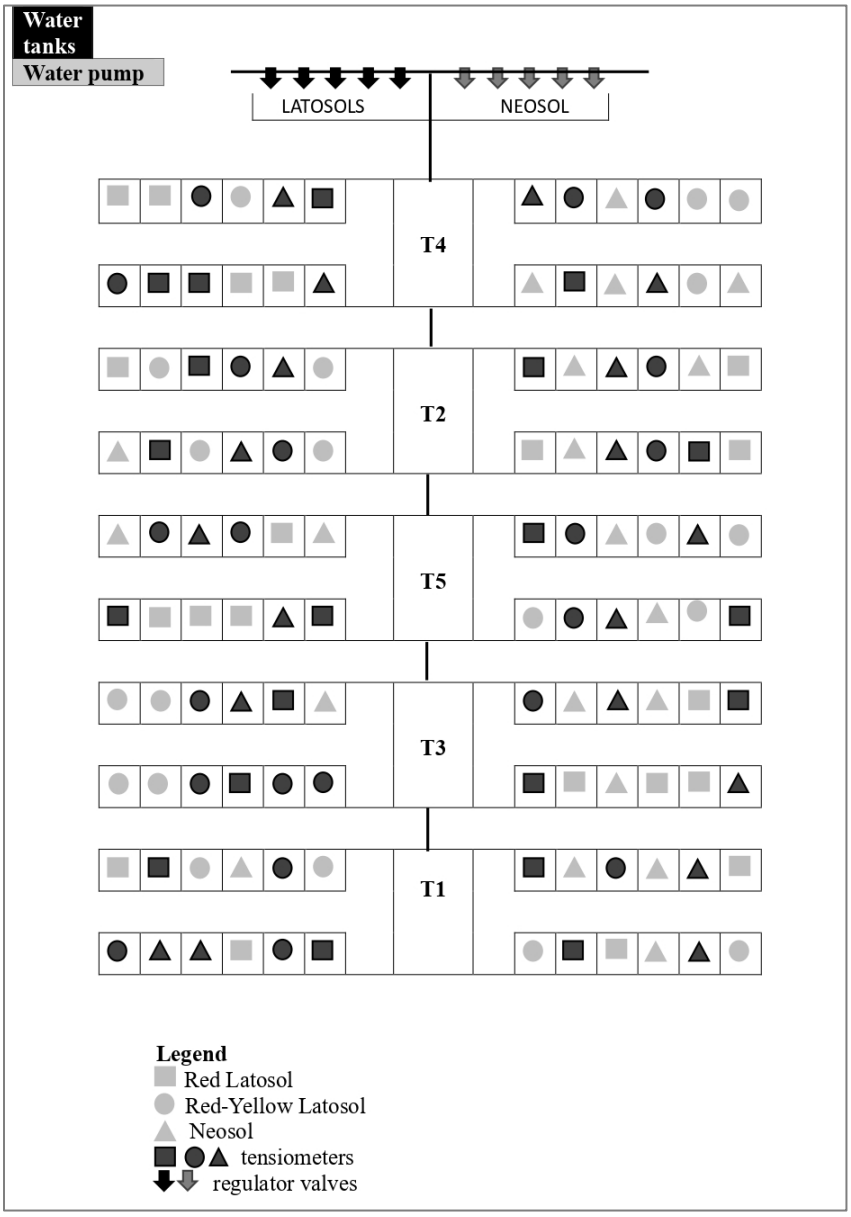

Figure 1. Experimental design in a controlled environment.

4.3 Monitoring the greenhouse's internal and external climate conditions

Climatological data during the crop cycle were obtained using a 900 ET WatchDog weather station (Spectrum Technologies) installed inside the greenhouse. The station can record air humidity, temperature, evapotranspiration (ET), solar radiation, wind speed and direction, wind chill, dew point and precipitation.

The SpecWare software allows to program data storage and download data according to user needs, showing the data in graphs and tables. Another feature of the software is that it can be used to calculate growing degree-days and chill hours, leaf wetness and temperature hours of relative humidity. In addition, it can provide daily, monthly and annual reports. Also,

this equipment has a digital LCD screen that displays parameters such as evapotranspiration, dew point and wind chill in real time.

4.4 Crop, cultivar, sowing and cultural practices

The common bean (*Phaseolus vulgaris* L.), cultivar BRSFC 104, which is produced by Embrapa, has a semi-precocious cycle of approximately 65 days, i.e., from sowing to grain maturation. This cultivar can reach an average yield of 3,792 kg ha^{-1}. It has moderate resistance to rust diseases, anthracnose and common bacterial blight (EMBRAPA, 2017).

Sowing was done on May 25th, 2021, at a depth of 3 cm. It was carried out in plastic pots with a volume of 11 L. On the inner base of each pot, we placed a synthetic non-woven mat and 2 cm of gravel was added over the mat for drainage. Four seeds were sown per pot, but only the two best plants were kept, corresponding to a total of 120 plants.

Control of weeds, pests and diseases was carried when necessary. The seeds were treated with the fungicide Maxim X, which contains active ingredients such as mefenoxam and fludioxonil. This included two applications of fungicide at days after emergence (DAE) 24 and 45. The fungicide contains the active ingredient mancozeb (750 g kg^{-1}). It was applied in solution at a concentration of 0,4 g L^{-1}. An insecticide with two active ingredients, i.e., deltamethrin (25 g L^{-1}) and neen oil, were also sprayed on DAE 39 and 34 at a concentration of 0.08 ml L^{-1} and 4 ml L^{-1}, respectively.

4.5 Physico-hydric and chemical characterization of soils

Sowing was carried out in three different types of soils, i.e., Red Latosol (Oxisol); Red-Yellow Latosol and Regolithic Neosol. The soils were first collected at Água Limpa Farm, FAV/UnB experimental field.

Following physical and chemical characterization of the soils (Tables 1 and 2), they were fertilized to correct pH and any nutrient imbalances according to Embrapa recommendations for Cerrado soils (SOUSA; LOBATO, 2004).

Fertilization was carried out manually in each pot, converting the amount recommended for a broadcast (field) application (in kg ha^{-1}) to a pot application representing a surface area of 530 cm^{-2} (g pot^{-1}) (Table 3).

For soil pH correction, magnesian limestone was used, whereas addition of potassium and phosphorus was done using potassium chloride (KCl) and Yoorin Master (P_2O_5) fertilizers.

Nitrogen was added in three applications, one at sowing and two at top-dressing using urea ($CO(NH_2)_2$) (Table 3).

Table 1. Particle size distribution, density (Ds) and porosity (Pt) of the first twenty centimeters of the Red Latosol, Red-Yellow Latosol and Regolithic Neosol.

Soil	Clay	Silt	Sand	Ds	Pt
	%	%	%	g cm^{-3}	cm^3 cm^{-3}
Red Latosol	72.7	25.1	2.20	0.94	0.64
Red-Yellow Latosol	59.2	36.7	4.10	1.00	0.62
Regolithic Neosol	14.3	8.60	77.2	1.28	0.51

Table 2. Chemical characteristics of the first twenty centimeters of the Red Latosol, Red-Yellow Latosol and Regolithic Neosol.

Characteristics	Red Latosol	Red-Yellow Latosol	Regolithic Neosol
pH	6.20	5.90	6.30
P	15.2	1.10	1.20
K	0.09	0.14	0.05
Ca	2.40	2.10	0.50
Mg	0.40	0.50	0.10
Na	0.11	0.15	0.03
Al	0.30	0.10	0.50
(H + Al)	3.40	3.20	3.00
BS	3.00	2.90	0.70
CEC	6.40	6.10	3.70
V	47.0	47.0	18.0
m	9.00	3.00	42.0
ISNa	4.00	5.00	4.00
C	20.0	11.0	4.50
MO	34.4	18.9	7.70

pH is in H_2O; P (Mehlich extractant), Ca, Mg, K, Na, Al are exchangeable phosphorus, calcium, magnesium, potassium, sodium and aluminum, respectively (cmol dm^{-3}); (H+Al) is exchangeable acidity (cmol dm^{-3}); SB is the sum of exchangeable cations (cmol dm^{-3}); CEC is cation exchange capacity (cmol dm^{-3}); V is base saturation (%) calculated as the sum of base cations Ca, Mg, K and Na on CEC; m is aluminum saturation (%) calculated a Al on CEC; ISNa is sodium saturation (%) calculated as Na on CEC; C is organic carbon (g kg^{-1}); and MO is organic matter (g kg^{-1}).

Table 3. Liming and fertilizer application rates by broadcast (field) per pots for the Red Latosol, Red-Yellow Latosol and Regolithic Neosol.

Nutrients	Recommendation (broadcast application, kg ha^{1})			Application per pot (g)			Sowing	Top-dressing	
								1^{st} application	2^{nd} application
	LR	LRY	RN	LR	LRY	RN			
Magnesian limestone	-	-	-	4.58	4.37	8.55			
N	100	100	100	1.16	1.16	1.16	20%	40%	40%
P_2O_5	150	420	320	1.88	13.2	10.0	100%	-	-
K_2O	60	100	125	1.18	0.72	0.96	60%	40%	-

LR: Red Latosol; LRY: Red-Yellow Latosol; and NR: Regolithic Neosol

4.6 Irrigation treatments, soil water tension and soil matric potential

The automated irrigation system consists of a water pump coupled to two 500 L water tanks. Irrigation was carried out using a drip system (i.e., dripper per button-type in each pot). The Regolithic Neosol has a coarser texture and in turn, it retains less water compared to the Red and Red-Yellow Latosols. For this reason, the irrigation system was composed of two regulator valve systems, one for the Latosols and one for The Neosol.

Flow rates were adjusted to create five soil matric potential for each soil type (see below for details). For the Latosols, soil matric potentials treatments were -10, -20, -25, -30 and -40 kPa, whereas treatments were -5, -10, -15, -20 and -25 kPa for the Neosol. In the first 22 days following seeding, however, all 60 pots received 3 minutes of irrigation at a nominal rate of 1 L h^{-1}. This procedure warranted seed germination and uniform seedlings before the onset of the water deficit treatments.

The measurement of soil matric potential started 18 days after seedling emergence. Soil matric potential was monitored using puncture tensiometers with a digital pressure gauge.

Soil matric potential was measured in all 60 pots at a 10 cm depth. Measurements were carried out on alternate days between 11:30 am and 13:30 pm. For each day, we were able to carry measurements of soil matric potential in 60 pots, i.e., 20 per soil type.

In this study we used the soil water retention curves (Figure 2) obtained by Pereira (2021) using the Van Genuchten (1980) model.

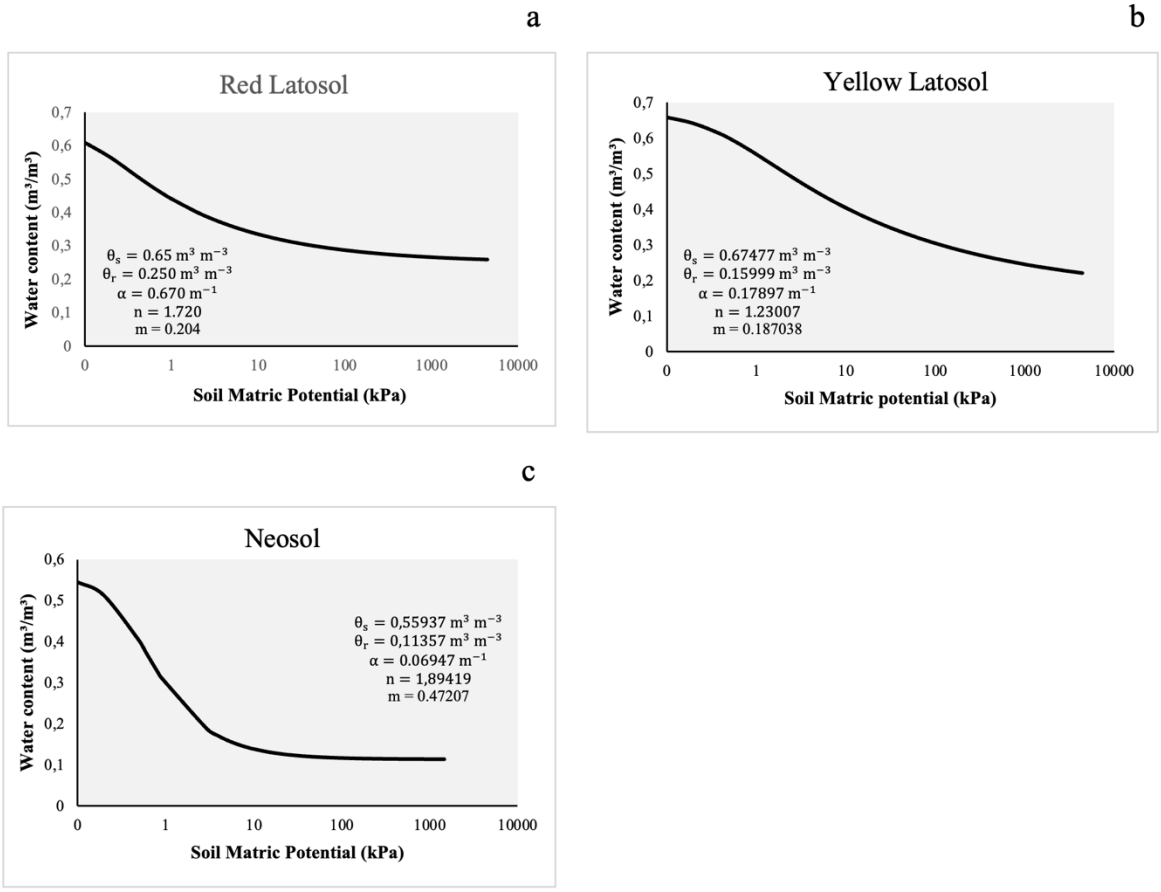

Figure 2. Soil water retention curves for the (a) Red Latosol, (b) Red-Yellow Latosol, and (c) Regolithic Neosol (Pereira, 2021).

The soil matric potential and water retention curves were then used to determine the water depts to be applied for each type of soil (Equation 1) and the time required to complete the application of these depths (Equation 2)

$$LI = (\theta\Psi - \theta)\, Z \qquad (1)$$

where

LI is the irrigation depth required to raise the soil moisture of the first twenty cm of soil to the field capacity or the soil water tension of interest (mm),

$\theta\Psi$ is the volumetric water content at the tension of interest for the first twenty cm of soil ($cm^3\ cm^{-3}$) obtained by using tensiometer and soil water retention curve,

θ is the estimated current volumetric water content for layer ten cm ($cm^3\ cm^{-3}$),

Z - Thickness of the layer at first twenty cm is the soil depth (mm).

$$TI = \frac{LI\ A}{Q\ Ea}\ 60 \qquad (2)$$

where

TI is the irrigation period (min),

LI is the irrigation depth required to raise the soil moisture of the first twenty cm of soil to the field capacity or the soil water tension of interest (mm),

A is the soil area per pot (m^2),

Q is the irrigation system flow rate (L h^{-1}), and

Ea is the application efficiency (decimal number).

4.7 Determination of leaf water potential (LWP)

The leaf water potential measurements were conducted at R8 (seed and pod filling stage). Leaf water potential (LWP) was obtained using the chilled-mirror dew point technique using a WP4-T Dewpoint Hygrometer (Decagon Devices). First, two leaf samples were removed from each plant. In total, we sampled 12 plants per block and 4 samples per soil type between DAE 47 and 66, for a total of 60 measurements.

The leaves were collected in the morning, stored in a sealed plastic bag and placed inside styrofoam to avoid water loss. The samples were brought quickly to the laboratory for analysis. A drop of distilled water was applied to the leaf surface after which a 600-grit fine sand paper was used to create a light abrasion of the leaf cuticle. Following this procedure, the leaf surface was cleaned thoroughly with a lint-free tissue to remove any excess water. Using a 40 mm diameter circular cutter, we then collected a sample of leaf tissue and placed it to cover the entire bottom of the 40 mm sample cup of the WP4 unit. The chamber was then quickly sealed to measure leaf water potential. These data were used to build a regression model between the CWSI, soil matric potential, and leaf water potential.

4.8 Determination of the Crop Water Stress Index (CWSI)

The Crop Water Stress Index (CWSI) was calculated using thermal images of the bean canopy. These images were obtained by a portable thermal camera (model DS-2TPH10-3AUF, Hikvision). The CWSI was determined according to the methodology proposed by Idso et al. (1981), which in summary considers the difference between the canopy temperature (T_c),

obtained by the thermal images, and the air temperature (T_a), obtained by the agroclimatological station (Equation 3).

Canopy temperature was measured on 60 plants, i.e., 20 samples per soil type, on alternate days between 11:30 am and 13:30 pm, for a total of 60 measurements.

$$CWSI = \frac{(T_c - T_a) - ((T_c - T_a)_{ll}}{(T_c - T_a)_{ul} - (T_c - T_a)_{ll}} \qquad (3)$$

where

T_c is the canopy temperature,

T_a is the average air temperature,

$(T_c - T_a)_{ll}$ is the non-water-stressed baseline (NWSB), corresponding to the air temperature difference for a crop without water deficit, i.e. when the resistance to water loss is zero or corresponding to the wet surface temperature, and

$(T_c - T_a)_{ul}$ is the upper temperature baseline, i.e. the non-transpiring baseline, corresponding to the air temperature difference when the canopy water loss resistance increases without limits or corresponding to the dry surface temperature.

The upper and lower temperatures were obtained by the maximum and minimum differences found between canopy temperature and air temperature (T_c-T_a).

The NWSB equation was obtained by linear regression of (T_c-T_a) against atmospheric vapor pressure deficit (VPD). The VPD was calculated using Equation 4.

$$VPD = 0.6108 * EXP\left(\frac{7.5 * T_a}{T_a + 237.3}\right) * \left(1 - \frac{RH}{100}\right) \qquad (4)$$

where,

RH is the relative humidity

4.9 Growth stages

The growth stages of the bean (Figure 4) ranged from EM - emergency day, V4 – vegetative stage between DAE 18 and 24, R5 and R6 - Floral induction and flowering between DAE 25 and 38, R7 – Pod formation between DAE 39 and 46, R8 - Seed and pod filling between DAE 47 and 66, and R9 - Physiological maturity between DAE 67 and 75. Note that the CWSI was not calculated only during the physiological maturity stage (R9).

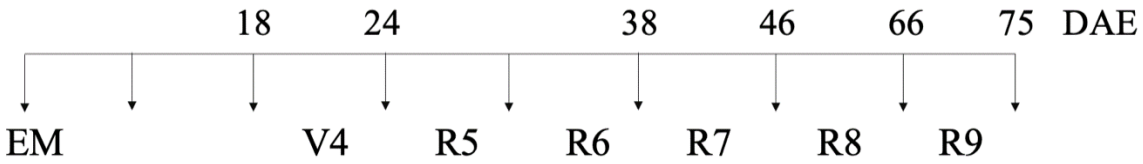

Figure 3: Growth stages of bean *Phaseolus vulgaris* L., cv BRSFC 104 cultivated in controlled environment.

In the initial growth stages, we had problems with the analogic pressure gauge, which later was changed to a digital pressure gauge with a silicone cap. We suspect that some tensiometers had small leaks, thus losing some vacuum inside the tensiometer. In addition, the extra cover of the greenhouse created some shading on the plants and thus reduced solar radiation inside. All these factors may have influenced the soil matric potential readings at V4, R5_R6 stages.

4.10 Mapping water stress using thermal image with UAVs

4.10.1 Aerial imagery and flight planning

To map the water stress in bean, the experiment was extended to another field in Luziania, located in the state of Goiás. Two sites were selected with Regolithic Neosol (16°19'03.0"S 47°52'39.8"W and 16°19'11.3"S 47°53'00.7"W). They were cultivated with bean crop and irrigated with in a center-pivot irrigation system. The bean was sowed on June 25th of 2021 at both sites. In these sites there was not measurement in situ of soil matric potential.

The thermal images were taken using a multirotor Unmanned Aerial Vehicle (UAV) (Table 4) using automated flights. More specifically, the flights were taken between 11:30pm and 14:30pm during days with a cloud-free sky, from 69 to 99 DAP (days after planting) using a Parrot ANAFI Thermal UAV. The UAV is equipped with a thermal camera (FLIR Lepton 3.5 microbolometer sensor) with a resolution of 160 pixels × 120 pixels. The sensor measures 7.5 to 13.5 μm spectral bands.

Automated flights were performed using Pix4DCapture, software. The UAV was programmed to fly at a ground speed of 1.5 m/s. Side lap and front-to-back overlap was set to 90% (the higher overlap, the lower the probability of errors, and the greater warranty that data are not missing in the processing of images). A flight altitude of 60 m above ground level (AGL) allowed a flight time of 20 minutes, whereas a Ground Sample Distance (GSD) of 1.67 cm was

used, considering the flight altitude and aiming to produce higher resolution imaging. On average, eight hundred images were collected per flight for the generation of each orthomosaic.

Table 4. Date, number and coordinates of flights, and number of plots of each flight for the bean crop.

Date	Dap	Number Of Flights	Coordinates	Number of plots
09/02/2021	69	1	16°19'03.0"S 47°52'39.8"W	3
09/04/2021	71	1	16°19'03.0"S 47°52'39.8"W	7
09/07/2021	74	1	16°19'03.0"S 47°52'39.8"W	6
09/11/2021	78	1	16°19'03.0"S 47°52'39.8"W	4
09/18/2021	85	1	16°19'03.0"S 47°52'39.8"W	4
09/21/2021	88	2	16°19'11.3"S 47°53'00.7"W	3
10/02/2021	99	1	16°19'11.3"S 47°53'00.7"W	5

4.10.2 Maps of thermal image-based crop stress indices

At first, the othormosaics for each flight were obtained using the PIX4D software. Using the tool raster extraction in QGIS, some representative plots, showed in Table 4, were selected from othormosaics to obtain the dry and wet references. The dry (T_{dry}) and wet (T_{wet}) canopy temperature were the average of the highest and lowest canopy temperature, respectively, of the histogram selected orthomosaic (Bian et al., 2019). This analysis was performed using the PCi Geometics software. These references were used to calculate the CWSI maps for each day.

The Crop Water Stress Index (CWSI) was calculated using canopy temperature of the bean obtained by the thermal camera coupled to the UAV. CWSI image maps were prepared using the raster calculator technique in QGIS 3.24. By doing so, it was thus was possible to have a CWSI value for each pixel of the image. The steps to create the maps are showed in Figure 3.

The CWSI was determined according to the methodology proposed by Idso et al. (1981), which considers the difference between the canopy temperature (T_c) and the lower and upper baselines (Equation 7). The CWSI was calculated using the raster calculation of QGIS.

$$CWSI = \frac{T_c - T_{wet}}{T_{dry} - T_{wet}} \quad (7)$$

where

T_c is the canopy temperature,

T_{dry} is the upper temperature baseline, i.e. the non-transpiring baseline, corresponding to the highest canopy temperature average of the orthomosaic histogram.

T_{wet} is the is the non-water-stressed baseline (NWSB), corresponding to the lowest canopy temperature average of the orthomosaic histogram.

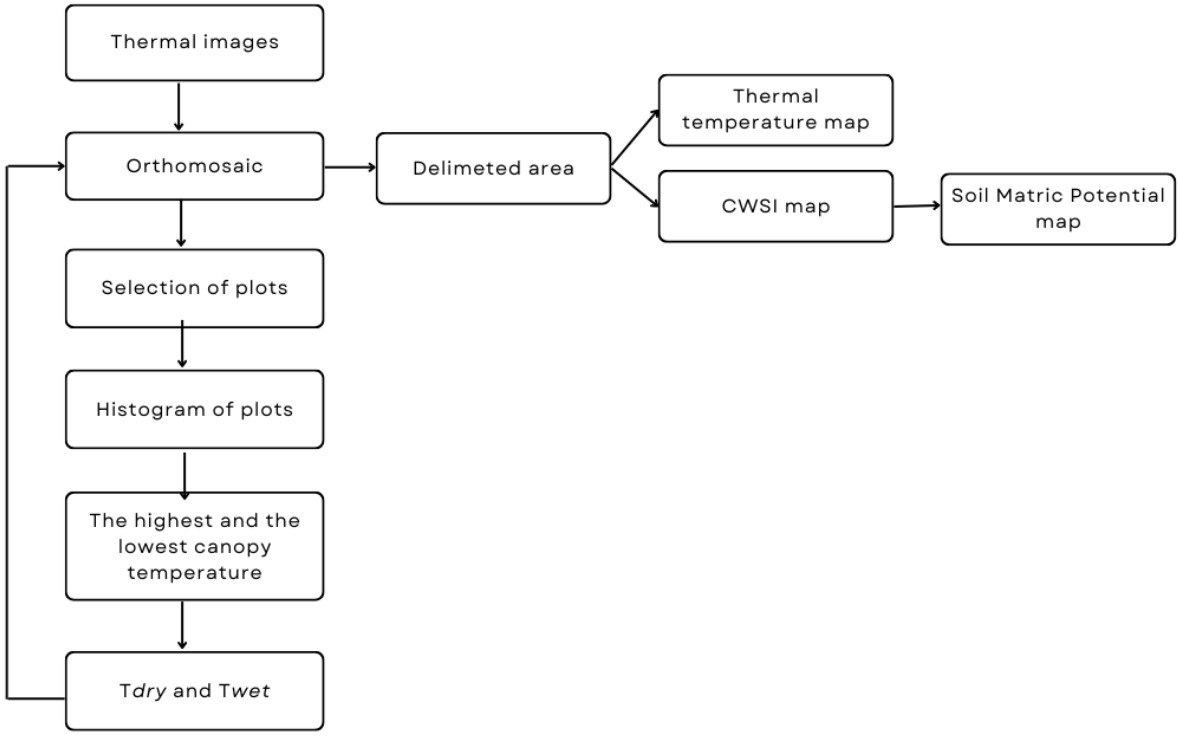

Figure 4: Flow chart to create the thermal temperature, CWSI and soil matric potential maps.

The soil matric potential was obtained from the regression equation at R8 stage for the Neosol: SMP = -188.84 $CWSI^2$ + 131.56 CWSI - 35.372 (R^2 = 0.96; p-value<0.05). This regression model calibrated in a controlled environment was used to predict the soil matric potential in the field with beans in a center-pivot and to develop water stress maps. The soil matric potential maps based on CWSI values were estimated using a raster calculator technique in QGIS 3.24.

4.11 Statistical analysis

Statistical software R was used for data analysis. The relationship between (Tc-Ta) versus VPD, and CWSI against soil matric potential and leaf water potential were analyzed through regression analysis, for that linear and non-linear regression models were developed using data collected under controlled conditions. The model performance and application were

evaluated using coefficient of determination(R^2), p-value, root mean square error (RSME) and the mean absolute error MAE.

5 RESULTS AND DISCUSSION

5.1 Lower baselines

The NWSB was obtained from the vegetative stage (V4) to the seed and pod filling stage (R8). The linear regression models of the lower baseline plotted against VPD for Red Latosol, Red-Yellow Latosol, and Neosol are showed in Figures 3, 4 and 5, respectively.

The Red-Yellow Latosol (R^2=0.62) and Regolithic Neosol (R^2=0,61) presented a relatively strong and significant (p-value<0,001) relationship between (Tc-Ta) and VPD, whereas the Red Latosol showed a weaker (R^2= 0.37) but yet significant (p-value ≤ 0.001) relationship. The VPD values ranged from 1.18 to 2.87 kPa. The canopy temperature and air temperature difference (Tc-Ta) ranged from -0.38 to -12.22 ◦C; 0.12 to -11.29 ◦C; and 0.12 to -11.99 ◦C for the Red Latosol, Red-Yellow Latosol and Regolithic Neosol, respectively.

In this experiment, were used climate data from 11:30 am to 13:30 pm. According to Erdem et al., (2006), the relationship can be affected by some factors such as clouds and wind, as well as incorrect readings of relative humidity. Many other factors such as cultivar, climatic conditions (including soil moisture), and growth stage also influence the upper baseline. In this respect, the different values in the regression equations developed for each soil type can be explained by the different capacities of these soils to retain and provide water for plant growth (KHORSAND et al., 2019).

Others studies also determined the lower baseline for bean crops around the world under no stress conditions, yielding the following models with some level of similarity: Tc-Ta=2.79-1.59VPD (Possignolo, Western Nebraska, 2020); Tc-Ta=2.91-2.35 VPD (Idso, 1982, Arizona); Tc-Ta=3.53-2.69 VPD (Erdem at al., 2006. Turkey); Tc-Ta=1.175-1.019 VPD (Asemanrafat and Honar, 2017, Iran). Some researchers state that the no stress baseline may be fitted better when it is determined for each growth stage of the crop, in order to represent precisely the difference of (Tc-Ta) against VPD. This requires to monitor the VPD and relative humidity over the growing season and then plot these data against (Tc-Ta).

The knowledge of water stress levels in plants by their growth stages may reduce the effects of water deficits on crop production, because water management can be done according to the need of the plant at each stage, and it can be managed in the earlier and later stages.

Lower availability of water in the reproductive stages as flowering and filling pods has a negative impact in crop production, the management of drought stress minimizes loss of productivity in the final stages, consequently, in yield. According to (Pradawet et al., 2021), water deficit in the initial stages of plants growth affects the plants height and leaf size, reducing photosynthesis rates. Whereas, water deficit in the final stages reduces yield, once the number of pods and the filling of grains are reduced.

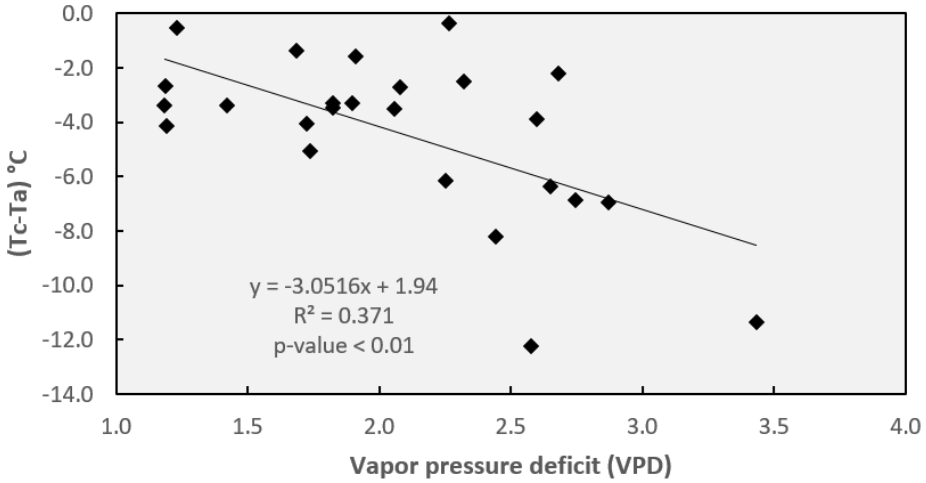

Figure 5. The non-water-stressed baseline (NWSB) for bean crop in the Red Latosol.

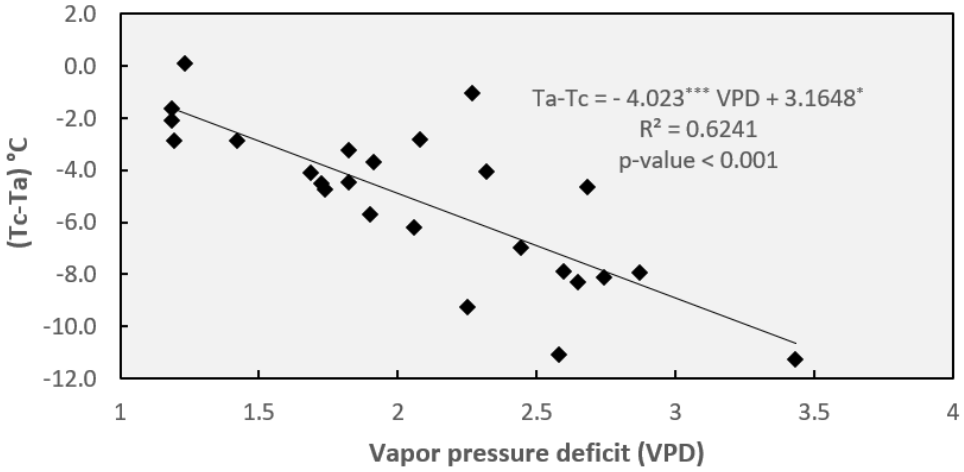

Figure 6. The non-water-stressed baseline (NWSB) for bean crop in the Red-Yellow Latosol.

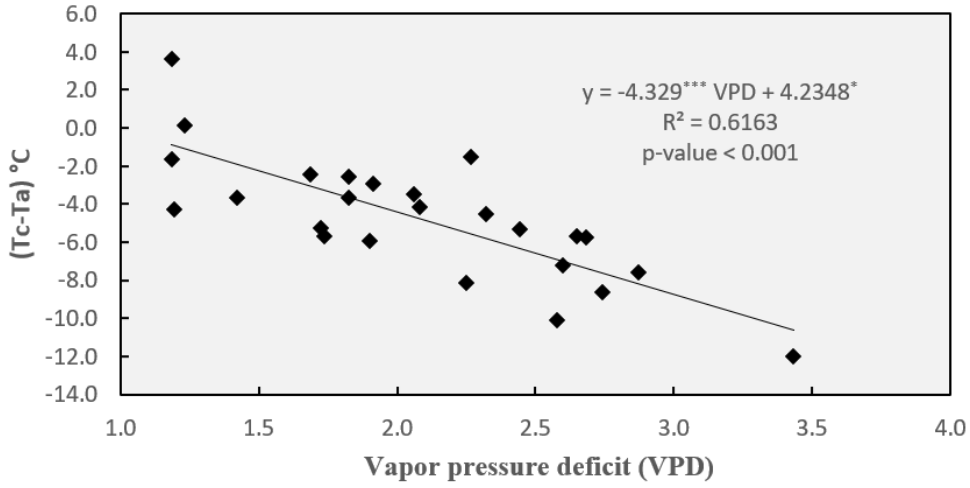

Figure 7. The non-water-stressed baseline (NWSB) for bean crop in the Regolithic Neosol.

5.2 Regression between CWSI and Soil Matric Potential

5.2.1 Red Latosol

Table 5 shows the R^2 and level of significance of the regression between the CWSI and soil matric potential for growth stages V4 to R8 of bean cultivated in the Red Latosol. Results suggest that regressions for V4, R5, R6 and R8 were not significant, whereas the regression was robust (R^2=0.8265) and significant (p-value = 0.032) for R7. For many of these models, here the low degrees of freedom likely explain the low statistical significance of the regressions.

Table 5. Regression results of CWSI yielded for the four growth stages of bean in the Red Latosol.

Growth Stage	Slops and intercept	R^2	F	p-value
V4	CWSI = 0.4898 SMP ^{2} + 5.5072 SMP + 15.8	0.5585	1.265 on 2 and 2 DF	0.4415
R5 and R6	CWSI = -0.1213 SMP ^{2} – 1.8359 SMP – 6.3056	0.7065	2.407 on 2 and 2 DF	0.2935
R7	CWSI = -0.0226 SMP – 0.145	0.8265	14.29 on 2 and 2 DF	0.0324
R8	CWSI = -0.003 SMP + 0.517	0.2517	0.3364 on 2 and 2 DF	0.7483

*Significant at $p \leq 0.05$

The results in general showed that CWSI and soil matric potential are correlated. The low availability of water in the soil resulted in high CWSI. The highest CWSI was estimated at

0.82 and was associated to the treatment with the most negative soil matric potential at R7 (Figure 8). This result corroborates with that of Silva et al., (2018) in tomatoes, where the treatments with the highest CWSI were found under water stress. The decrease in soil water content is the likely cause, as the plant reduces its transpiration by partially or totally closing its stomata. As a consequence, the canopy temperature tended to increase, and CWSI is the evidence. In general, a decrease in soil water content will tend to increase CWSI values, especially if air temperature and plant transpiration are measured near or at their peaks, e.g., at noon (XU et al., 2016)

For R5 and R6 stages, the relationship between the CWSI and soil matric potential was not significant, but the lowest CWSI value (0.20) was estimated in the treatment with the less negative soil matric potential (Figure 8). The coefficient of determination was also high (R^2=0.70). Because soil moisture in this treatment was high and in turn, canopy temperature was low (or equilibrated), this result can be considered as evidence for an unstressed crop plant in regard to water. According to Xu et al., (2016), under conditions where the CWSI value of rice was low and the plants did not suffer from water stress, soil water availability was sufficient to satisfy the plant's physiological processes. This particular state was reflected by low to moderate air temperature and thus relatively low water losses from evapotranspiration.

The prediction of SMP in response to CWSI is showed in Table 6, a significant relation was observed at stage R7 (R^2=0.84 and $p<0.05$). The relation was weak and not significant for V4 and R5 and R6, and R8 stages.

Table 6. SMP prediction in response to CWSI for the four growth stages of bean in the Red Latosol.

Growth Stage	**Slops and intercept**	**R^2**	**p-value**
V4	SMP = -10.554 CWSI ^{2} + 7.5979 CWSI – 6.9136	0.5136	> 0.05
R5 and R6	SMP = 7.349 CWSI ^{2} – 10.602 CWSI – 4.0059	0.4969	> 0.05
R7	SMP = 27.826 CWSI ^{2} – 63.067 CWSI – 5.0416	0.8486	< 0.05
R8	SMP = 786.58 CWSI ^{2} – 1058.2 CWSI + 321.76	0.3148	> 0.05

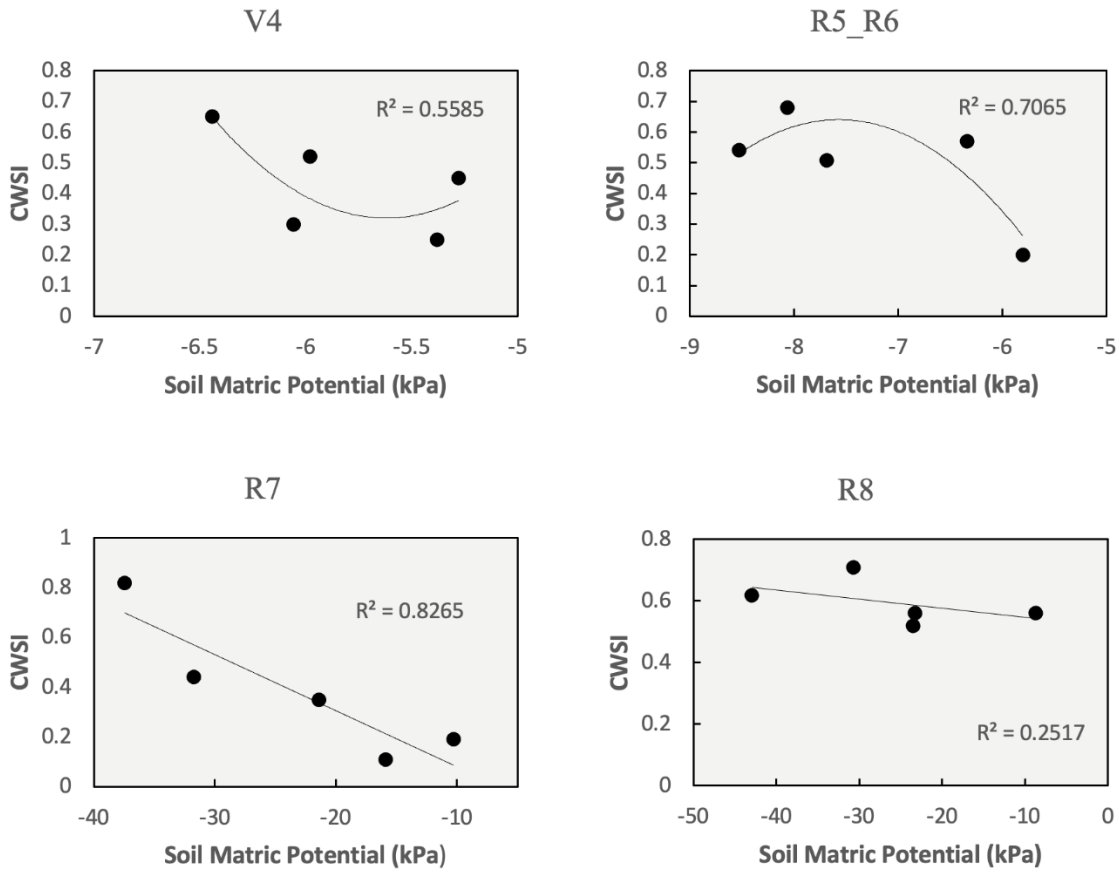

Figure 8. The CWSI plotted against the soil matric potential at different growth stages for bean in the Red Latosol. V4 represents the vegetative stage, R5_R6 represent the flowering stage, R7 represents the pod formation stage, and R8 represents the seed and pod filling stage.

5.2.2 Red-Yellow Latosol

The regression between CWSI and soil matric potential for the various growth stages of bean cultivated in the Red-Yellow Latosol are presented in Table 7. We computed very strong and significant regressions at stages R5 and R6 (R^2=0.8566; p-value < 0.05) R7 (R^2=0.9795; p-value<0.05) and R8 (R^2=0.9596; p-value < 0.05). For stages V4, coefficient was high (respectively R^2=0.8354), but due to the low degrees of freedom, they were not statically significant.

Table 7. Regression results of CWSI yielded for the four growth stages of bean in the Red-Yellow Latosol.

Growth Stage	Slops and intercept	R^2	F-statistic	p-value
V4	CWSI = 0.5174 SMP^2 + 5.8972 SMP + 16.929	0.8354	5.074 (3 and 1 DF)	0.1646
R5 and R6	CWSI = 0.0519 SMP^2 + 1.0162 SMP + 5.042	0.8566	17.97 (1 and 3 DF)	0.0240
R7	CWSI = 0.0003 SMP^2 - 0.0102 SMP - 0.1531	0.9795	47.84 on 2 and 2 DF	0.0205
R8	CWSI = -0.0013 SMP^2 - 0.0936 SMP - 1.0083	0.9596	23.77 on 2 and 2 DF	0.0404

*Significant at $p \leq 0.05$

At the R5 and R6 stages the highest CWSI value (0.84) was found in the treatment with the lowest soil water content (Figure 9). The lowest and the highest CWSI values at stage R7 were respectively estimated under the lowest and the highest soil matric potential treatments, i.e. 0.07 and 0.69 (Figure 9). At the R8 stage, the lowest CSWI value was 0.19 and this was also related to the highest soil matric potential (Figure 9). These, CWSI results at R5 to R8 suggest that canopy temperature is sensitive to soil water availability, i.e., when water availability decreases, leaf temperature increases. The same observations between CWSI and canopy temperature under an irrigation gradient were made by Quiloango-Chimarro et al., (2020) in common beans. Our results also corroborate with Heydari et al., (2019) and Bijanzadeh et al., (2022) who found, for canola and sunflower crops, respectively, the lowest CWSI values under the irrigated treatment and the highest values under the water stress treatment.

Table 8 shows SMP prediction equations in response to CWSI, a very strong and significant coefficient of determination was observed at R8 stage ($R^2 = 0.98$ and p-value<0.05). Whereas, V4, R5 and R6, and R7 showed good coefficient of determination ($R^2 > 0.62$), but they were not significant (p-value<0.05).

Table 8. SMP prediction in response to CWSI for the four growth stages of bean in the Red-Yellow Latosol.

Growth Stage	Slops and intercept	R^2	p-value
V4	SMP = 23.137 CWSI ^{2} – 18.107 CWSI – 2.7391	0.8453	> 0.05
R5 and R6	SMP = -24.071 CWSI ^{2} + 17.604 CWSI – 11.187	0.6221	> 0.05
R7	SMP = 21.072 CWSI ^{2} – 52.946 CWSI – 11.497	0.9856	< 0.05
R8	SMP = 25.82 CWSI ^{2} – 59.382 CWSI – 6.6149	0.7332	> 0.05

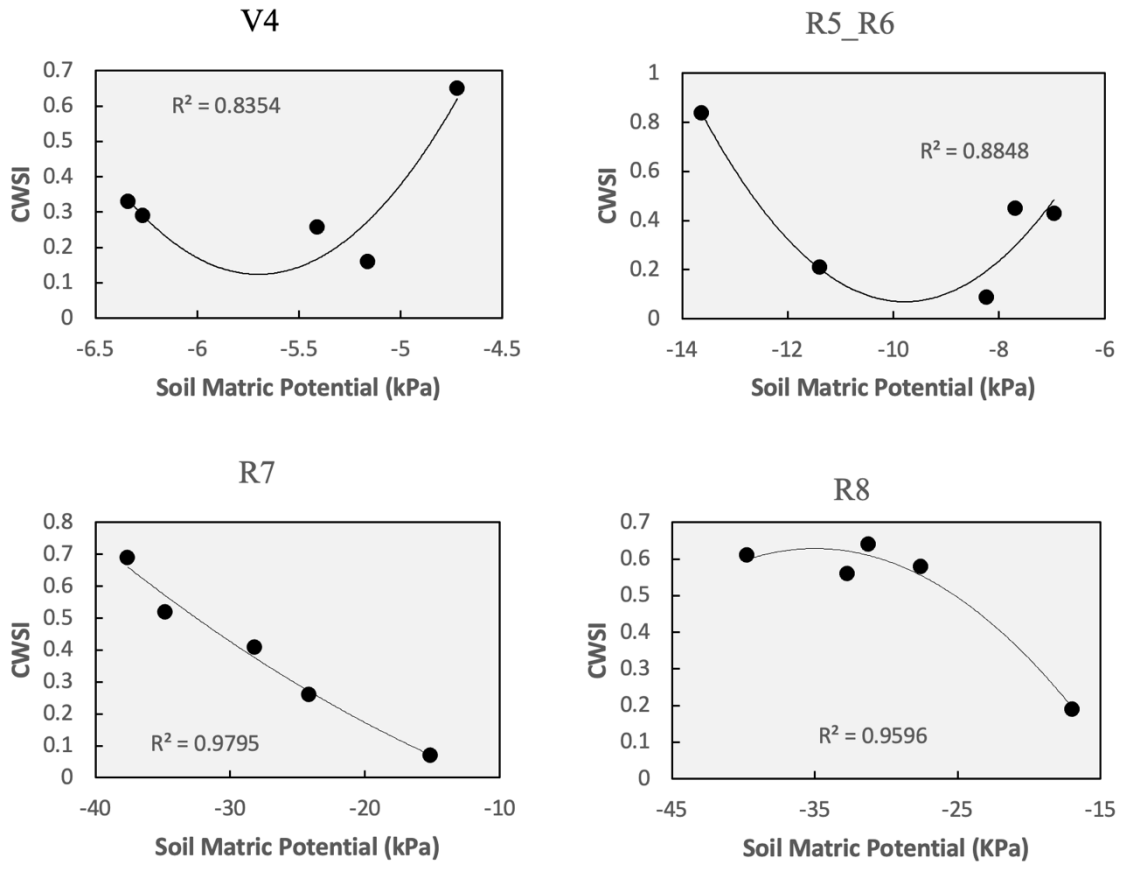

Figure 9. The CWSI plotted against the soil matric potential at different growth stages for bean in the Red-Yellow Latosol. V4 represents the vegetative stage, R5_R6 represent the flowering stage, R7 represents the pod formation stage, and R8) represents the seed and pod filling stage.

5.2.3 Regolithic Neosol

For the Regolithic Neosol, regressions between CWSI and soil matric potential were very strong (R^2>0.95) and significant only at stages V4 and R8 (p-value < 0.05) (Table 9). For

both stages R7 and R8, the lowest and the highest CWSI values are associated to the highest and lowest soil matric potential, respectively. More specifically, for the R8 stage, the very dry treatment (-20kPa) had the highest CWSI value and the highest soil moisture treatment (-5kPa) had the lowest CWSI value. At the R7 stage, the lowest CWSI values was 0.15 and the highest was 0.78, whereas these values were 0.3 and 0.65, respectively, for R8 stage (Figure 10). Nouri at al., (2020) observed that the relationship between CWSI and soil moisture in bean crops under different irrigation treatments was negative and significant. The highest value of CWSI was found under the treatment representing the more severe water stress, i.e., the treatment with less irrigation, whereas the lowest CWSI value was found in the treatment receiving full irrigation.

Table 9. Regression results of CWSI yielded for the four growth stages of bean in the Regolithic Neosol.

Growth Stage	Slops and intercept	R^2	F	p-value
V4	CWSI = -0.1953 SMP^2 - 2.5551 SMP - 7.9466	0.9566	22.05 on 2 and 2 DF	0.0434
R5 and R6	CWSI = -0.0086 SMP^2 - 0.2778 SMP - 1.4397	0.6744	2.072 on 2 and 2 DF	0.3256
R7	CWSI = -0.0013 SMP^2 - 0.0717 SMP - 0.3105	0.5109	1.045 on 2 and 2 DF	0.4891
R8	CWSI = -0.0015 SMP^2 - 0.0848 SMP - 0.5317	0.96818	30.36 on 2 and 2 DF	0.0319

*Significant at $p \leq 0.05$

At R7, and R5 and R6 stages, there was no significant relationship between CWSI and soil matric potential, but again, the highest CWSI value (0.73) was estimated in the treatment with the lowest soil water content (Figure 10). According to Asemanrafat and Honar, (2017), the CWSI is conducive to change under different treatments, and CWSI is also affected by irrigation depths. They found that the treatments closest to field capacity of the soil should have CWSI values closer to zero as result of the regular supply of water. Under conditions of water stress, however, CWSI values should tend towards a value of 1.

The capability of CWSI predict SMP was significantly strong at R8 (R^2=0.96, p-value<0.05) (Table 10). The coefficient of determination was weak for V4, R5 and R6, and R7 stages.

Table 10. SMP prediction in response to CWSI for the four growth stages of bean in the Regolithic Neosol.

Growth Stage	Slops and intercept	R^2	p-value
V4	SMP = - 44.089 $CWSI^2$ + 26.666 CWSI – 10.5	0.335	> 0.05
R5 and R6	SMP = - 16.316 $CWSI^2$ + 2.5963 CWSI – 8.1761	0.498	> 0.05
R7	SMP = 31.694 $CWSI^2$ – 51.935 CWSI – 3.575	0.440	> 0.05
R8	SMP = - 188.84 $CWSI^2$ + 131.56 CWSI – 35.372	0.96	< 0.05

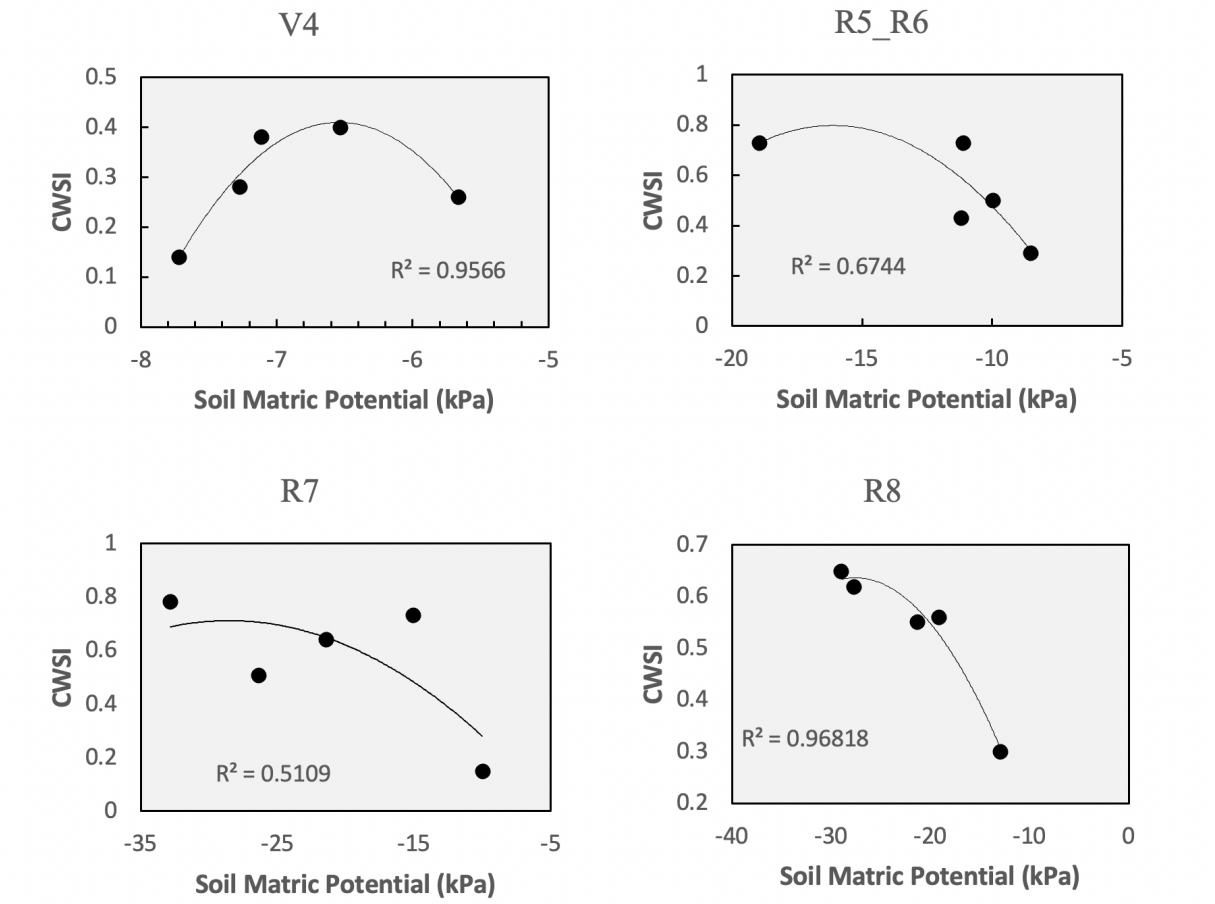

Figure 10. The CWSI plotted against the soil matric potential at different growth stages for bean in the Regolithic Neosol. V4 represents the vegetative stage, R5_R6 represent the flowering stage, R7 represents the pod formation stage, and R8) represents the seed and pod filling stage.

5.3 Regression between CWSI, Soil Matric Potential and Leaf Water Potential

The regressions between CWSI and leaf water potential for the Red Latosol, Red-Yellow Latosol and Neosol are showed in Figure 9. For the Red Latosol (R^2=0.87) and Neosol (R^2=0.92) the regression was strong, while for the Yellow-Red Latosol the relation was weak, but not significant (p-value >0.05) for all soil types in this study.

According to our results, CWSI increases as LWP decreases which is consistent with the results of Chastain et al., (2016) and Shellie and King (2020). For the Red Latosol (Figure 11a), Red-Yellow Latosol (Figure 11b), and Regolithic Neosol (Figure 11c), the treatments under irrigation deficit showed the lowest values of leaf water potential, which are associated with the highest CWSI values. These results corroborate with those found by Kirnak et al., (2019) who observed that the relation between CWSI and LWP for pumpkin was strong (R^2= 0.98 in 2015 and R^2=0.96 in 2016). Wijewardana et al., (2019) reported that the LWP decreased as the soil moisture decreased.

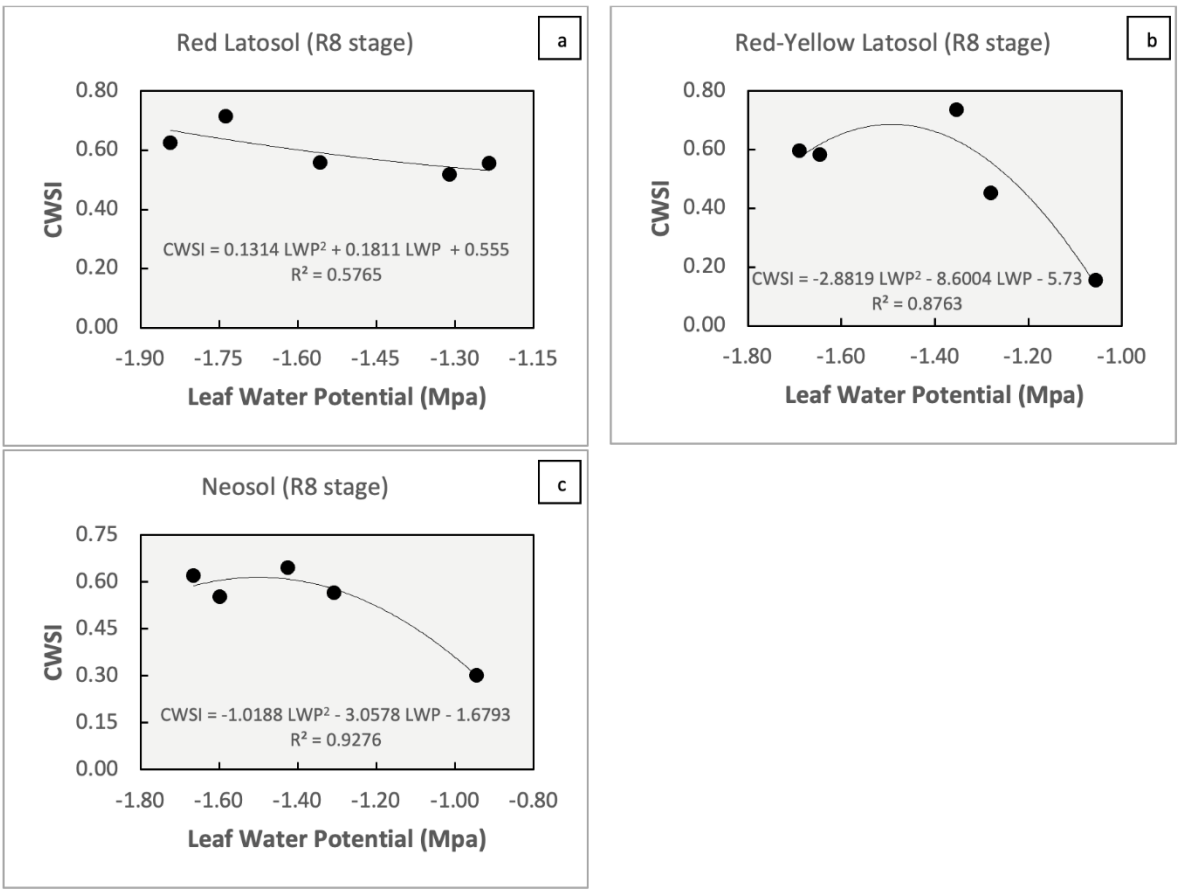

Figure 11. The CWSI against Leaf Water Potential at R8 stage for bean in different soil types: (a) Red Latosol, (b) Red-Yellow Latosol, and (c) Regolithic Neosol.

The multiple regression equations were extracted for the parameters of CWSI, soil matric potential and leaf water potential, in order to better understand these relations of plant and soil indices with CWSI. The results showed a good relationship for all studied soils, for the Red Latosol (R^2=0.69), the Red Yellow (R^2=0.75) and the Neosol (R^2=0.97), but none the regressions were significant (p-value > 0.05). Table 11 shows the models for predicting CWSI for the Red Latosol, Yellow-Red Latosol and Neosol in response LWP.

Table 11. Multiple regressions models and multiple R-squared for predicting CWSI at phase R8 in beans.

Type of soil	Models	R^2
Red Latosol	CWSI = 0.0751951 - 0.0057555 * SMP - 0.4241548 * LWP - 0.0003614 * SMP * LWP	0.69
Red Yellow Latosol	CWSI = -0.271972 + 0.021511 * SMP - 0.261347 * LWP + 0.007366 *SMP * LWP	0.77
Regolithic Neosol	CWSI = - 0.79520 -0.06174 * SMP -0.77416 * LWP - 0.03473 SMP * LWP	0.97

5.4 Mapping water stress and application of CWSI to predict soil matric potential in bean

Canopy temperature was the based index to calculate CWSI and SMP, as showed in Figures 10a to 16a, by thermal temperature of canopy in bean. The canopy temperature ranged from 20.57 to 44.06 °C (Figures 13a to Figures 19a). It was possible to use thermal-based images and equations developed from a field cultivated with the same crop, soil and climate conditions to detect water stress in bean plants. Ekinzog et al. (2022) used the relationship obtained between CWSI and soil moisture to create soil moisture maps.

The results showed that SMP prediction using CWSI at R8 stage for the Neosol were strongly correlated with soil matric potential measured in controlled conditions with coefficient of determination (R^2=0.85), RMSE=3.08, MAE=2.34, and p-value <0.05 (Figure 12). The relationship between CWSI measured in the controlled environment and the one measured in the field was significant (R^2>0.78; RMSE and MAE =0.07, p-value<0.05). The CWSI measured in the field and the soil matric potential predicted was significant correlated with R^2=0.97, RMSE=23.86, MAE= 22.65, and p-value<0.05 (Table 12).

The prediction regression models in this study demonstrated the higher applicability of CWSI to monitor the levels of stress in plants, manly, when correlated to SMP. The strong relation obtained between the indices measured in the controlled conditions and in field conditions has evidenced the CWSI as precisely method to be used in determining water status in plants for later stages of growth and mapping of drought stress and spatial availability of water in the soil. Studies have been showing effectiveness plant predictions based on calibrated models in a controlled environment (Pradawet et al., 2022), and how it can lead to improve crop water management for different crops, soil and climate conditions. In a controlled environment the monitoring the plants, soil and climate parameters can be done according to given purposes

for different scenarios, i.e, assessing water stress applying different irrigation depths, at growth stages, periods of the day, reducing the meteorological influences, once it is calibrated and validated can be used in fields as a reliable method.

To analyze the spatial variability of the water status in bean, for each flight, CWSI and soil matric potential (SMP) maps were generated. These are shown in Figures 13 to 26, which are representative of 69, 71, 74, 78, 85, 88 and 99 days after planting (DAP). The CWSI ranged from 0.0055 to 1 (Figures 13b to 19b). The values close to 0 indicate the area under no water stress, whereas the values close to 1 indicate water stress. The CWSI values obtained in our study can be used to identify the well irrigated and poorly irrigated areas as well as the spatial variability of water stress in the field.

The thermal image-based soil matric potential map showed the variation of water content levels in the same the field (Figures 20a to 26a), among different plots (Figures 20b to 26b). On DAP 71 and 78, CWSI and SMP values were at their highest (CWSI = 0.62 and 0.63, and SMP = 29.82 and -34.39 kPa), respectively, meaning that these areas were more susceptible to water stress. On DAP 88 showed the less variation in water availability, as evidenced by the lower CWSI and SMP average, 0.36 and -13.36kPa (Table 13).

In our study, the maps of soil matric potential showed a fairly large spatial variability in soil water content. The soil matric potential ranged from -12,45 to -93 kPa. Similarly, for two years of study, Banerjee et al., (2020) found that variation in soil water content changed depending of water stress treatments. These results allowed to understand the dynamics of water in plants and in the soil in the entire area of study, and how mapping can identify spatial variations in water status in the field for different areas or plots.

In our study, distinct variation in soil water availability was found in all thermal image-based maps of CWSI and soil matric potential. On DAP 69, SMP in plot 1 ranged from -12.45 to -71.47 kPa, and from -12.45 to -93 kPa for plots 2 and 3. Plot 3 was more sensitive to water stress and had less soil water availability as indicated by higher CWSI values and more negative SMP values. On DAP 71, SMP in plots 1 and 3 ranged from -12,45 to -93kPa, and from -13.66 to -93kPa for plot 2. Plot 3 showed less susceptivity to water deficit and in fact, it showed higher water availability. For Dap 74, the SMP in plots 1 and 2 ranged from -12.45 to -93 kPa and from -12.45 to -71.22 kPa, respectively. Plot 1 showed more water availability with less negative SMP values. On DAP 78, SMP in all plots (1, 2 and 3) ranged from -12.45 to -93 kPa. Plots 1 and 2 showed more negative SMP values and higher CWSI values, indicating a water deficit. On DAP 85, SMP in plot 1 ranged from -12,45 to -81.97 kPa, and from -12.45 to -75.22 kPa and -12.45 to -85.32 kPa in plots 2 and 3, respectively. On DAP 85, plots 1 and 2

were less sensitive to water stress compared to plot 3, but in each of these plots, we observed a substantial variation in water content. On DAP 88, SMP in plot 1 ranged from -12.45 to -68.90 kPa, and from -12.45 to -48.33 kPa in plot 2. CWSI and SMP showed less variation and this can likely be attributed to an adequate supply of water in the field. On DAP 99, SMP ranged from -12.45 to -93kPa in plot 1, -12.45 to -31.75 kPa in plot 2, and -12.45 to -33.52 kPa in plot 3. Which variation patterns indicate that plot 1 was more susceptible to water stress with higher CWSI values and more negative SMP values. These results can be used to apply different irrigation rate in the field, optimize the irrigation scheduling, avoiding both under-irrigation and over-irrigation. Moreover, precision irrigation practices enable the most accurate water management in agricultural fields, maximizing crop yield and reducing costs.

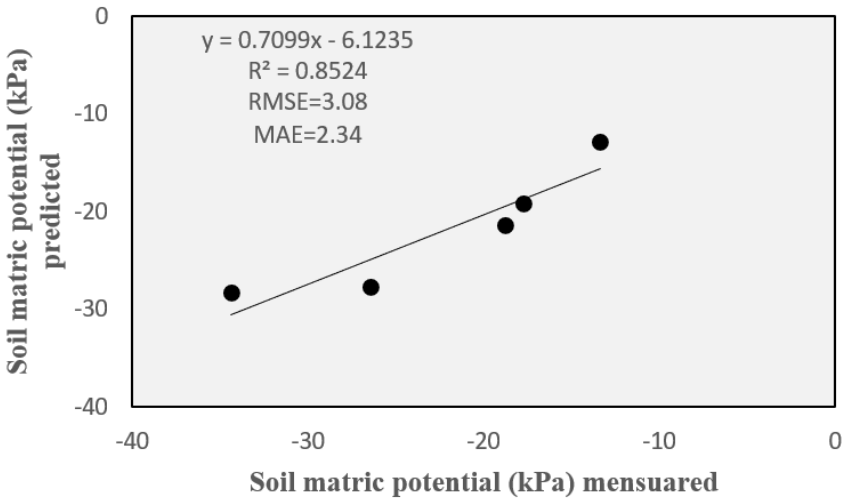

Figure 12. Application of the linear regression between SMP computed in a controlled environment and SMP obtained in the field (center pivot) at R8 stage of bean for the Regolithic Neosol.

Table 12. Relationship between water stress indices CWSI and SMP measured in a controlled environmental and predict in a field.

	Regression models	R^2	p-value	RMSE	MAE
SMPc x SMPp	SMPp = -0.7098x + 6.1244	0.852	0.025	3.08	2.34
CWSI x CWSIs	CWSIs = 1.2286x - 0.066	0.785	0.045	0.076	0.07
CWSIs x SMPc	SMPc = -133.02x^2 + 50.995x - 14.153	0.976	0.024	23.86	22.65

SMPc: soil matric potential measured in a controlled environment; SMPp: soil matric potential predicted in a field; CWSI: empiric; CWSIs: using dry and wet references.

Table 13. Average of CWSI and soil matric potential (kPa) for selected plots cultivated with bean in the Regolithic Neosol predicted in the field.

	CWSI			Soil Matric Potential (kPa)				
DAP	Plot 1	Plot 2	Plot 3	Plot 1	Plot 2	Plot 3	Average CWSI	Average SMP
69	0.45	0.49	0.56	-16.17	-16.82	-23.04	0.50	-18.68
71	0.69	0.66	0.52	-36.14	-32.22	-21.09	0.62	-29.82
74	0.35	0.55	-	-13.68	-21.93	-	0.45	-17.81
78	0.71	0.75	0.43	-38.54	-47.65	-16.99	0.63	-34.39
85	0.44	0.39	0.55	-17.08	-15.46	-24.11	0.46	-18.88
88	0.37	0.34	-	-13.47	-13.31	-	0.36	-13.39
99	0.68	0.18	0.44	-35.82	-18.09	-15.26	0.43	-23.06

Overall, the higher values of CWSI corresponded to the areas where the soil water content was lower, and this was demonstrated by the more negative soil matric potential. Conversely, the lower values of CWSI were obtained in the areas where soil water availability was greater and this was demonstrated by less negative soil matric potential. These results are corroborated by Ekinzog et al. (2022) where the CWSI maps were efficient in showing the variation in water stress levels. The spatial variability of CWSI in our study was well coupled to the spatial variability of soil matric potential (Figures 13 to 26). Similarly, Bian et al, (2019) found that CWSI maps were a robust fit with soil water content under different irrigated treatments, and provided evidence that CWSI can indicate water stress in cotton. Banerjee et al., (2020) used thermal image-based maps to assess water stress in wheat and its spatial variability. They found that the higher values of CWSI were in the plots where plants were more susceptibility to water stress, whereas the lower CWSI was measured in plants and areas with less susceptibility to water stress. It confirms the suitable relationship between canopy temperature and soil moisture (Vieira and Ferrarezi, 2021), although in this study, soil moisture was represented by the soil matric potential.

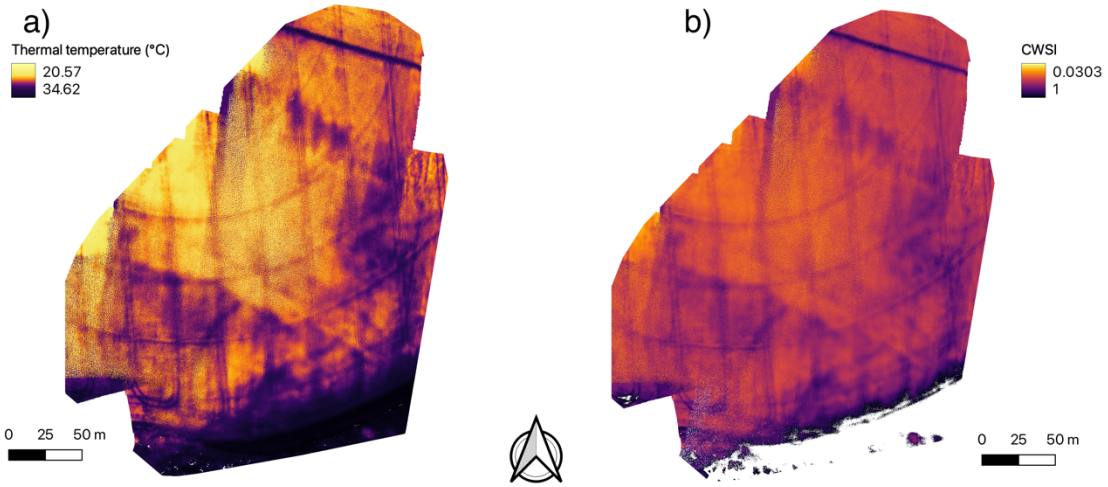

Figure 13. (a) Thermal temperature map; (b) CWSI map of beans of *Phaseolus vulgaris* 69 days after planting.

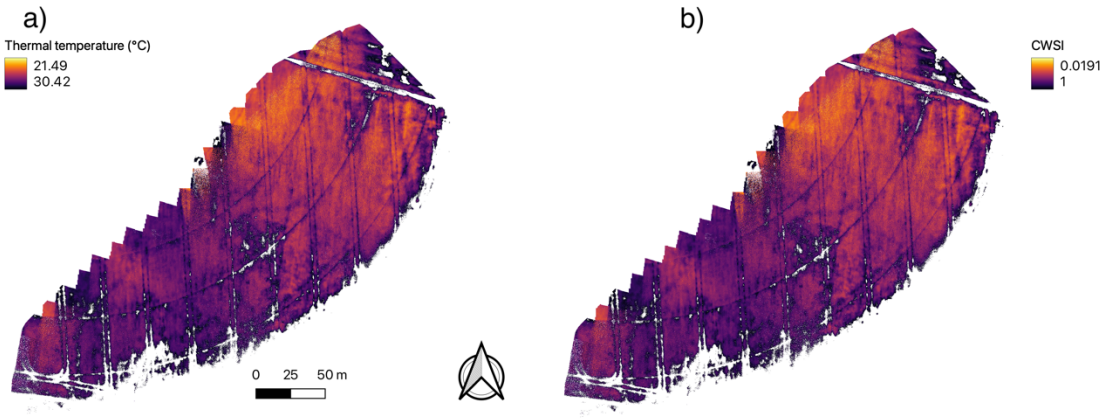

Figure 14. (a) Thermal temperature map; (b) CWSI map of beans of *Phaseolus vulgaris* 71 days after planting.

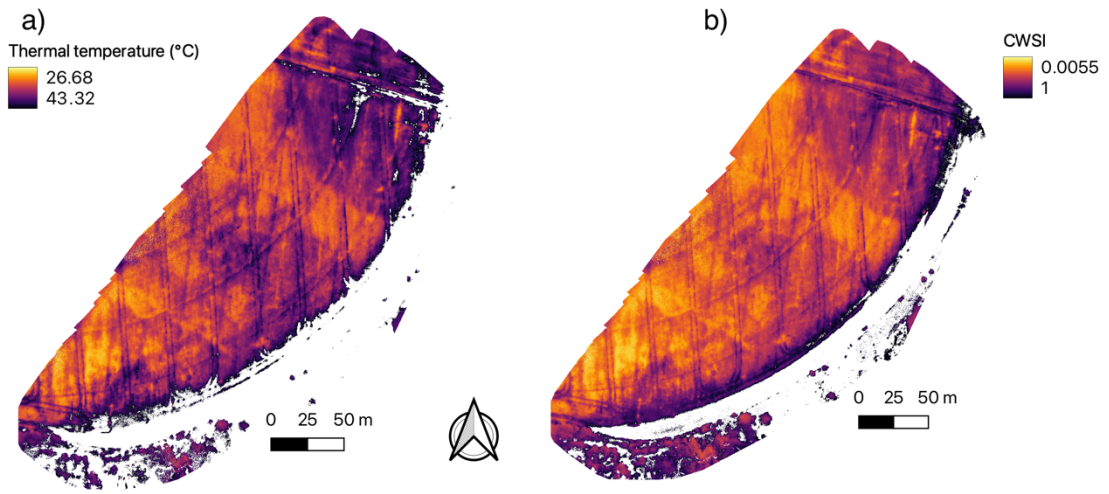

Figure 15. (a) Thermal temperature map; (b) CWSI map of beans of *Phaseolus vulgaris* 74 days after planting.

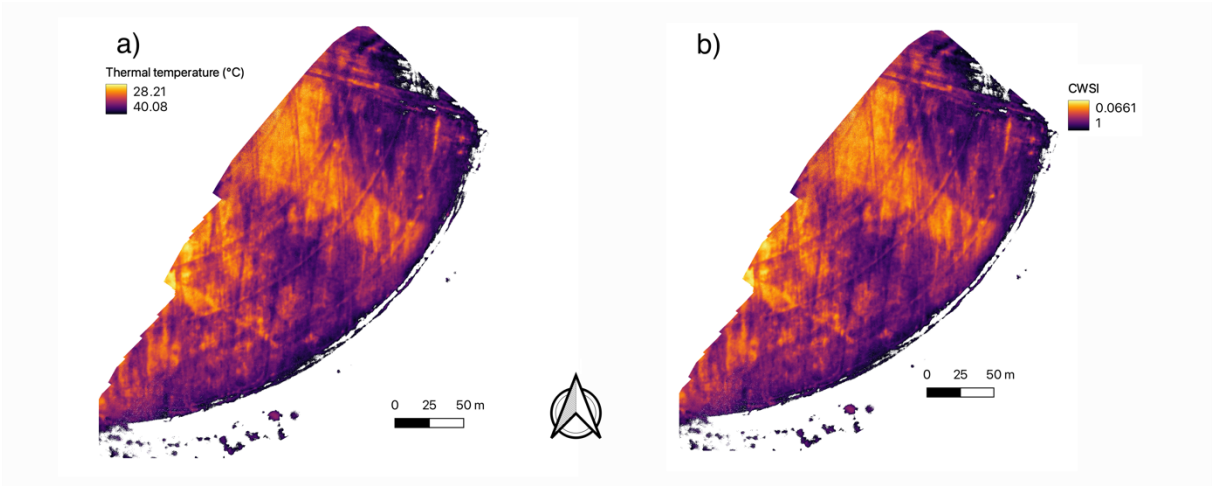

Figure 16. (a) Thermal temperature map; (b) CWSI map of beans of *Phaseolus vulgaris* 78 days after planting.

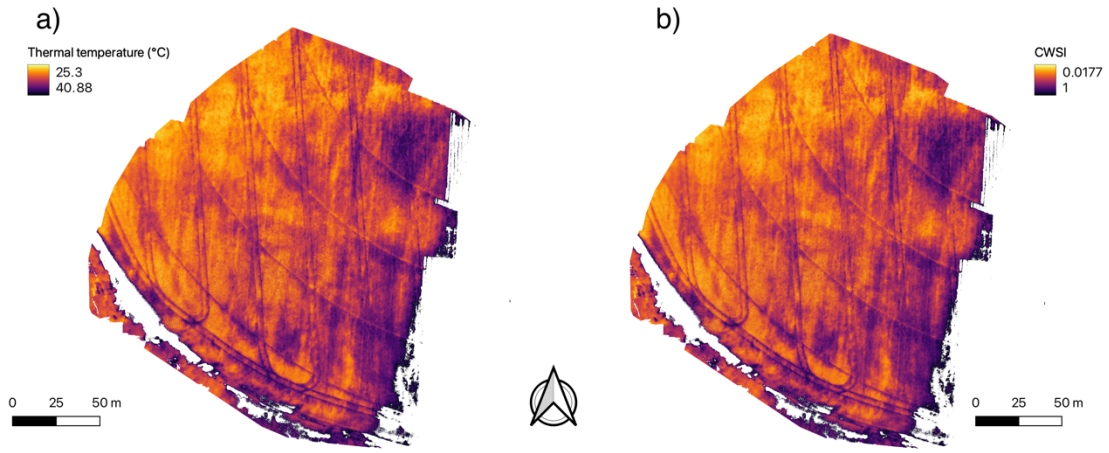

Figure 17.(a) Thermal temperature map; (b) CWSI map of beans of *Phaseolus vulgaris* 85 days after planting.

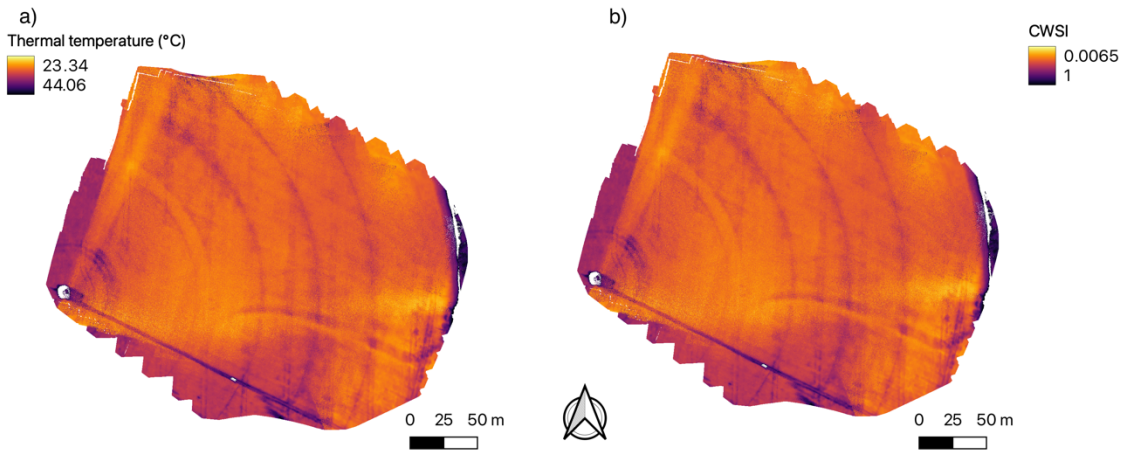

Figure 18. (a) Thermal temperature map; (b) CWSI map of beans of *Phaseolus vulgaris* 88 days after planting.

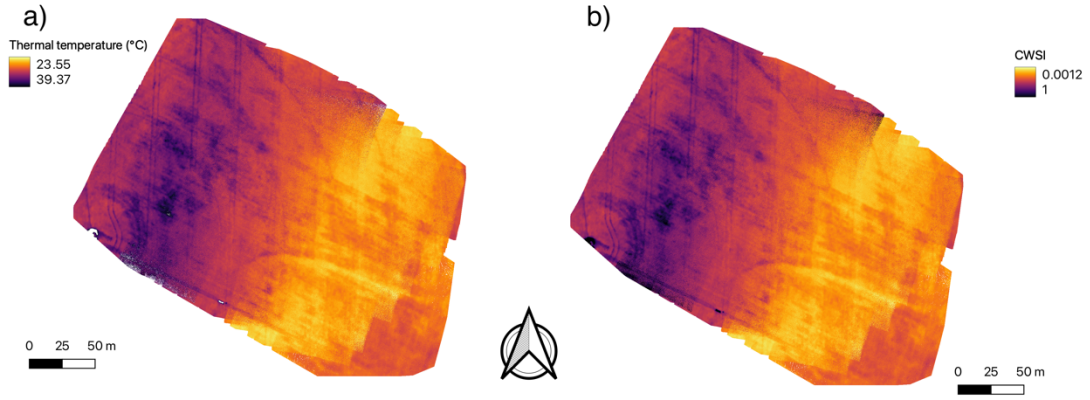

Figure 19. (a) Thermal temperature map; (b) CWSI map of beans of *Phaseolus vulgaris* 99 days after planting.

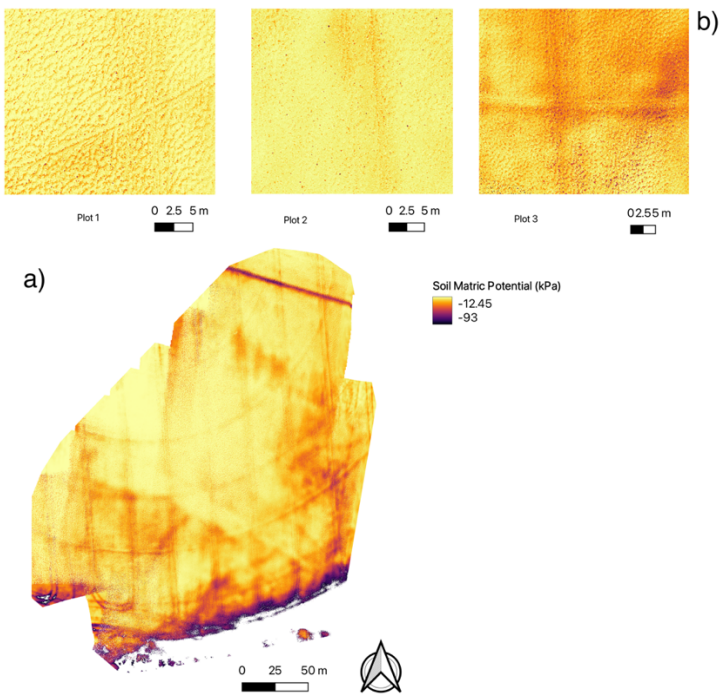

Figure 20 (a) Soil matric potential map; and (b) Soil Matric potential for plots 1, 2 and 3 of beans of *Phaseolus vulgaris* 69 days after planting.

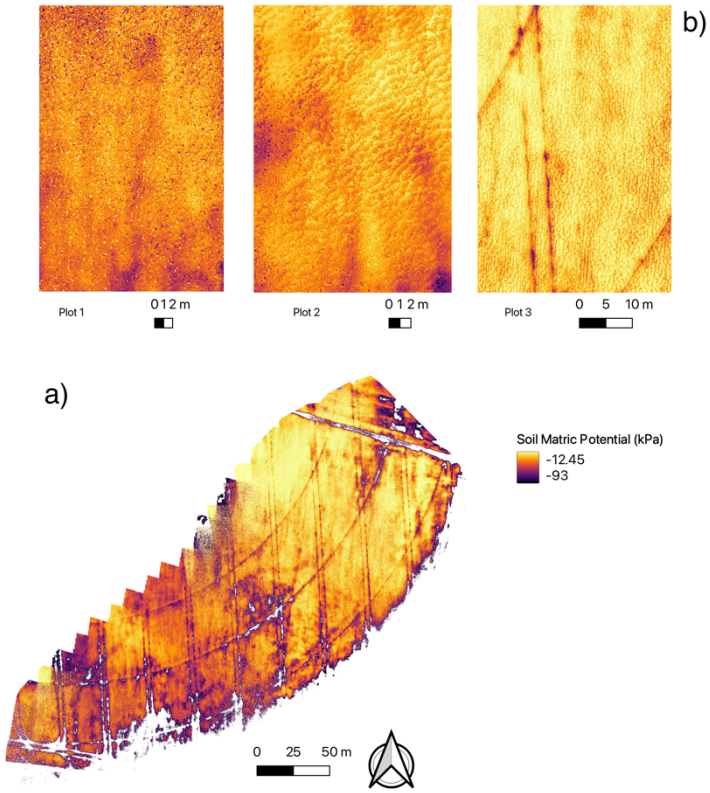

Figure 21. (a) Soil matric potential map; and (b) Soil matric potential for plots 1, 2 and 3 of beans of *Phaseolus vulgaris* 71 days after planting.

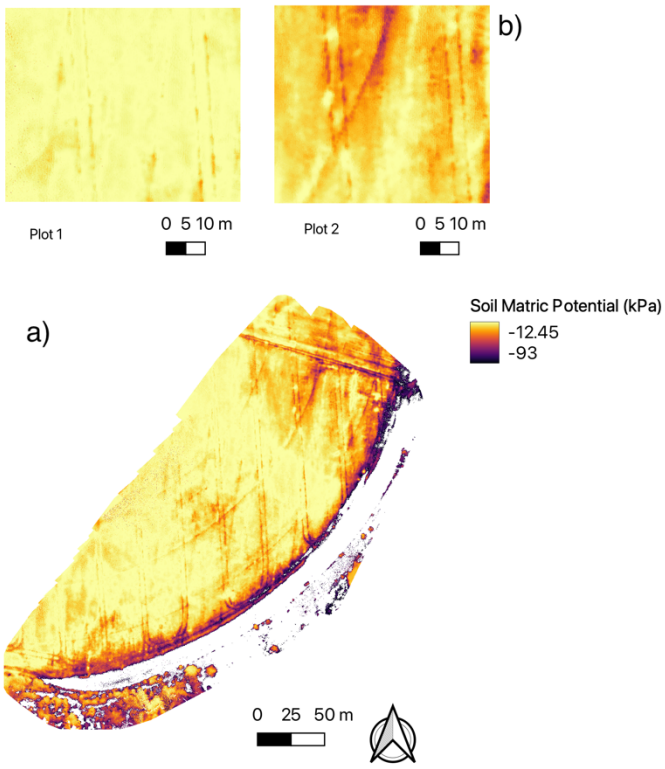

Figure 22. (a) Soil matric potential map; and (b) Soil matric potential for plots 1, 2 and 3 of beans of *Phaseolus vulgaris* 74 days after planting.

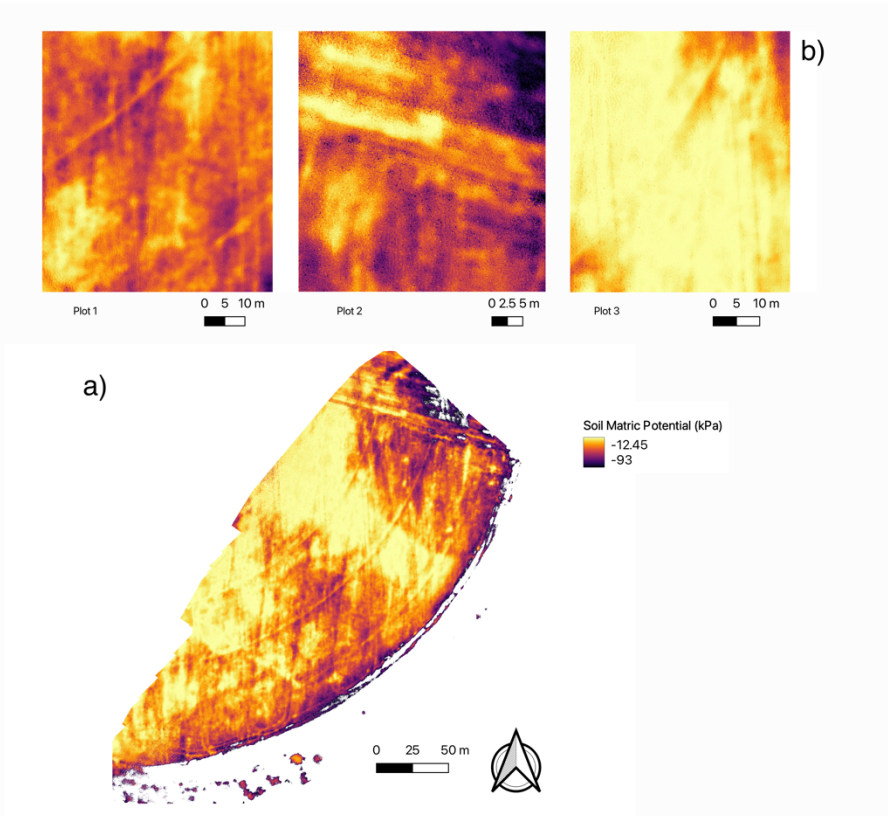

Figure 23. (a) Soil matric potential map; and (b) Soil matric potential for plots 1, 2 and 3 of beans of *Phaseolus vulgaris* 78 days after planting.

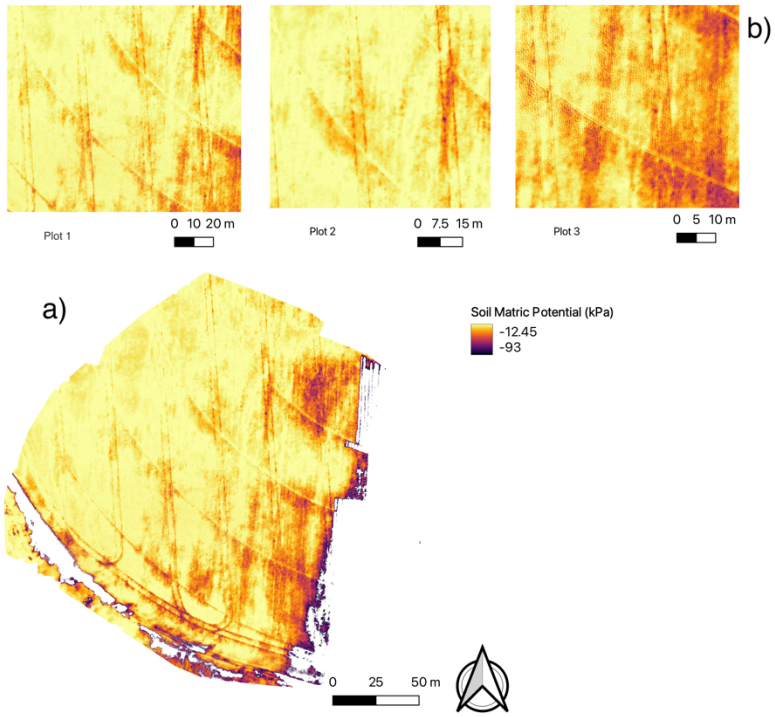

Figure 24. (a) Soil matric potential map; and (b) Soil matric potential for plots 1, 2 and 3 of beans of *Phaseolus vulgaris* 85 days after planting.

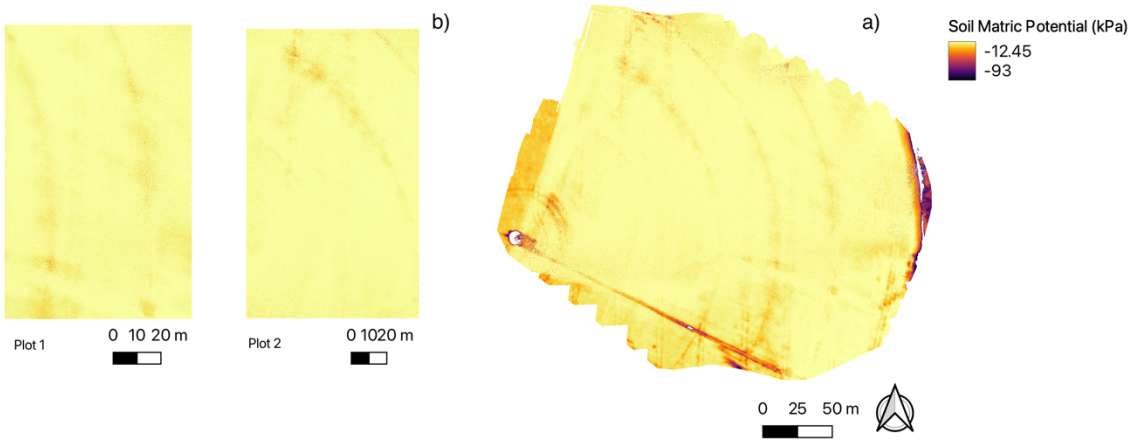

Figure 25. (a) Soil matric potential map; and (b) Soil matric potential for plots 1, 2 and 3 of beans of *Phaseolus vulgaris* 88 days after planting.

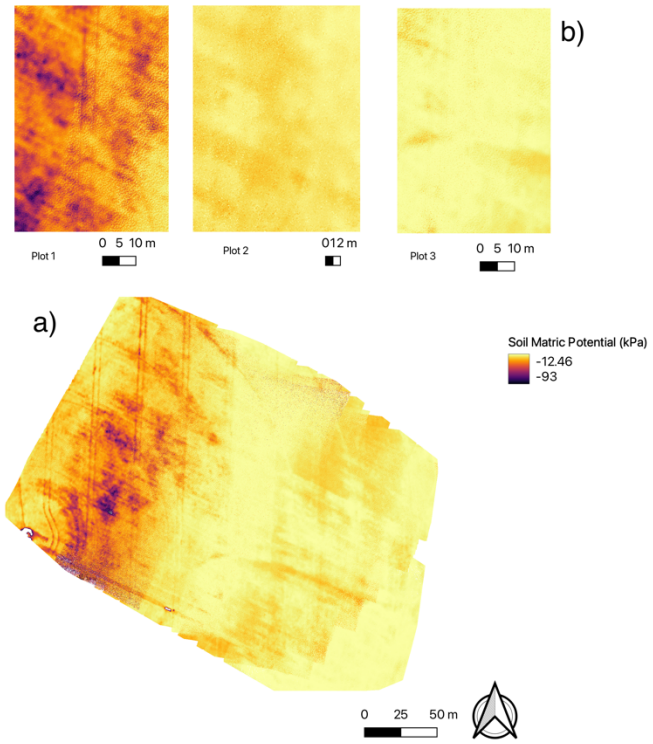

Figure 26. (a) Soil matric potential map; and (b) Soil matric potential for plots 1, 2 and 3 of beans of *Phaseolus vulgaris* 99 days after planting.

Considering our results of mapping water stress, irrigation zones can be identified and variation rates of irrigation van be applied. Indeed, results suggest that applying different amounts of water in the field at different rates considering the local demand is likely a good strategy to both satisfy the plant's specific needs and reduce water use. As such, irrigation scheduling management can be done based on variation in soil water content in the field. According to Vieira and Ferrarezi (2021), canopy temperature threshold is required to determine the time at which plants should be irrigated as well as the depth irrigation should be applied. In this respect, soil water content assessed through thermal mapping can be an effective method. Moreover, the advantages of using thermal images captured form UAVs are that an extensive area can be mapped in a short period of time. Concurrently, measurements in the filed can be done during flights.

Our results support the idea that the characterization of spatial variability in soil water content and water stress in plants can help farmers improve the management of irrigation scheduling in bean, mainly in large scale. At the current time, the timing and rates of irrigation are not defined with enough precision and that is due to the difficulties in monitoring the crop in the entire field. Mapping of soil matric potential allows to determine the amount and timing of irrigation at a given CWSI. When the thermal-based images maps are combined with plant

stress indicators, they can be used as a means to improve the crop water efficiency and the precision of irrigation. Thus, is crucial to understand the water relations in plants and crop water stress levels, the advantages of using UAV thermal imaging to monitor stress include less energy, fuel and water consumed by plants.

5.5 Considerations about the methodology

In this study, the exclusion of the soil pixels visible in the background, with no canopy cover, was not done, but boundaries where there was not canopy cover was not compute as thermal temperature. When plots have complete canopy closure with no soil visible in the background, the application of CWSI in the field also appears more robust because only canopy temperature is measured. According to Bian et al., (2019), the traditional methods to remove soil pixels from images are complex and expensive.

The experiment in the field did not have any measurement in situ such as soil matric potential or leaf water potential. Soil matric potential values were estimated based on the model obtained in the controlled environment and on the canopy temperature of the plants in the field. Also, the research did not explore a canopy temperature threshold which irrigation needs to be applied, a range where any change in CWSI does not cause stress in plants. The predicted SMP in the field was close to -93kPa in some plots, in the controlled environment we did not compute such value of soil matric potential, but we have established a soil matric potential (-25kPa) threshold, the CWSI and crop stress condition at this given soil matric potential value is known. When the measurement reaches the critical soil matric potential value, it means that irrigation needs to be provided for plants.

The most suitable period to obtain thermal imagery is around midday on days of clean sky, on cloudless days, it allows a more precisely detection in water stress. Moreover, empiric CWSI is easy to obtain, it only requires the canopy temperature and air temperature, in windy conditions the canopy temperature tends to decreased, but when the soil is dry, the lower canopy temperature cannot properly respond to stress condition. An alternative solution is to use the theorical CWSI, which requires not only air temperature as well as wind speed, relative humidity and solar radiation. Furthermore, studies may be applied to compare the empirical and theorical to estimate the accuracy of them.

Additionally, the selection of plots based on their temperature variation was an efficient method to compute the lowest and highest thermal canopy temperature. The simplified CWSI is easy to compute, once dry and wet references are obtained from the canopy temperature

histogram, besides that the canopy temperature is derived from a thermal image. On the other hand, the simplified approach of CWSI is more applicable for farmers in the field because it requires less data. Other researchers have shown that CWSI yielded from canopy temperature histograms is a reliable and simple approach to measure CWSI (PARK, 2017, 2021; BIAN, 2019). Bian et al., (2019), also suggest that the CWSI calculated from canopy temperature histograms reduces errors occurring during manual measurements and due to the influence of meteorological factors. Crusiol et al., (2019) used the lowest and highest canopy temperature from a field trail to asses water stress in plants, the thermal images were taken under the same climate and weather conditions, thus these reference values proved a reliable representation of transpiration conditions of plants.

6 CONCLUSION

The CWSI based on canopy temperature appears to be an effective tool to determine the need of irrigation in bean considering its growth stages. In this study, significant curvi-linear regressions between the soil matric potential and CWSI were found for the Red Latosol at growth stage R7; for the Yellow-Red Latosol at stages R5 to R8; and for Regolithic Neosol at stages V4 and R8. These results demonstrated good relationship between CWSI and soil matric potential, and the capability of prediction of soil matric potential using CWSI.

Prediction equations can be used to estimate the CWSI and soil matric potential as a means to monitor water deficit in plants. These can be used to better define irrigation needs in beans and thus develop more precise irrigation management plans. The results showed the potential of CWSI predict SMP for the Red and Yellow Latosols at R7, whereas for the Regolithic Neosol at R8. When calibrated in controlled conditions by a plant water indicator such as the leaf water potential and soil matric potential, the CWSI can be used to predict water stress in plants and be used as an indicator for scheduling irrigation and water management in agriculture, mainly in areas where there are limitations for site measurements.

Canopy temperature images were effective to predict the CWSI and soil matric potential. The CWSI and soil matric potential maps were able to identify the areas where levels of water stress in bean low or high. In this study, soil matric potential had better performance when correlated with CWSI than leaf water potential. However, further studies are required to remove the soil pixels of thermal images, which are a significant source of uncertainties during calculation of a proxy of soil water availability.

Thermal images were able to estimate soil moisture, which shows that thermal image obtained from UAVs is a reliable method for precision irrigation, helping farmers in a more efficient irrigation management of cultivated areas. Additionally, it is a non-destructive and rapidly method to determine soil moisture when compared to the traditional ones. Moreover, farmers can apply the UAV and traditional methods together, making them more reliable.

7 REFERENCES

ALCHANATIS, V; COHEN, Y; COHEN, S; MOLLER, M.; SPRINSTIN, M.; MERON, M.; TSIPRIS, J., SARANGA, Y; SELA, E. Evaluation of different approaches for estimating and mapping crop water status in cotton with thermal imaging. **Precision Agriculture**, v.11, p.27-41, 2010.

AL-KARADSHEH, E., SOURELL, H.; KRAUSE, R. Precision Irrigation: New strategy irrigation water management. Conference on International Research on Food Security, Natural Resource Management and Rural Development, Deutscher Tropentag, Witzenhausen, p.11-22, 2002.

ALGHORY, A., YAZAR, A. Evaluation of crop water stress index and leaf water potential for deficit irrigation management of sprinkler-irrigated wheat. Irrigat. Sci. 37, p.61–77, 2019.

ALI, H.; IQBAL, N; SHAHZAD, A.N.; AHMAD, S.; KHAN, Z.M; SARWAR, N. Agro-management practices for sustainable wheat production under scarce water condition of arid climate. **Turk Journal Field Crops**, v.19, p.70–78, 2014.

ASEMANRAFAT, M., HONAR, T. Effect of water stress and plant density on canopy temperature, yield components and protein concentration of red bean (*Phaseolus vulgaris* L. cv. Akhtar). **International Journal of Plant Production**, 11(2), 2017.

ARGYROKASTRITIS, I.G; PAPASTYLIANOU, P.T; ALEXANDRIS, S. Leaf Water Potential and Crop Water Stress Index variation for full and deficit irrigated cotton in Mediterranean conditions. **Agriculture and Agricultural Science Procedia**, v.4, p.463–470, 2015.

BALLESTER, C. et al. Usefulness of thermography for plant water stress detection in citrus and persimmon trees. **Agricultural and Forest Meteorology**, v. 168, p. 120-129, 2013.

BANERJEE, KOUSHIK; P. KRISHNAN, P; DAS, BAPPA. Thermal imaging and multivariate techniques for characterizing and screening wheat genotypes under water stress condition. **Ecological Indicators**, v.119, 106829, 2020.

BELLVERT, J.; MARSAL, J.; GIRONA, J.; GONZALEZ-DUGO, V.; FERERES, E., USTIN, S.L.; ZARCO-TEJADA, P.J. Airborne thermal imagery to detect the seasonal evolution of crop water status in peach, nectarine and Saturn peach orchards. **Remote Sensing**, v.8, p.1-17, 2016.

BIAN, J; ZHANG, Z; CHEN, J; CHEN, H; CUI, C; LI, X; CHEN, S; FU, Q. Simplified Evaluation of Cotton Water Stress Using High Resolution Unmanned Aerial Vehicle Thermal Imagery. **Remote Sens**, 11, 267, 2019. doi:10.3390/rs11030267

BIJANZADEH, E; MOOSAVI, M.M; BAHADORI, F. Quantifying water stress of safflower (Carthamus tinctorius L.) cultivars by crop water stress index under different irrigation regimes. **Heliyon,** V.8, Issue 3, March 2022. https://doi.org/10.1016/j.heliyon.2022.e09010

BILSKIE, J. Soil water status: content and potential. 2001. Campbell Scientific, Inc. Available on:<http://s.campbellsci.com/documents/cn/technical-papers/soilh20c.pdf>. Access on jul. 1st, o2021.

CAMPOS, K; SCHWEMBER, A. R; MACHADO, D.; OZORES-HAMPTON, M.; GIL, P.M. Physiological and Yield Responses of Green-Shelled Beans (*Phaseolus vulgaris* L.) Grown under Restricted Irrigation. **Agronomy**, 11,562, 2021. https://doi.org/10.3390/agronomy11030562

CARDOSO, M. R. D.; MARCUZZO, F. F. N.; BARROS, J. R. Classificação climática de Köppen-Geiger para o Estado de Goiás e o Distrito Federal. ACTA Geográfica, v.8, n.16, p.40-55, 2014.

CHASTAIN, D. R; SNIDER, J. L; COLLINS, G. D.; PERRY, C. D.; WHITAKER, J.; BYRD, S. A.; OOSTERHUIS, D. M.; PORTER, W. M. Irrigation Scheduling Using Predawn Leaf

Water Potential Improves Water Productivity in Drip-Irrigated Cotton. Crop science Vol. 56, p.3185–3195, 2016. doi: 10.2135/cropsci2016.01.0009

CHEN, J.; LIN, L.; LÜ, G. An index of soil drought intensity and degree: an application on corn and a comparison with CWSI. **Agricultural Water Management**, v.97, p.865–871, 2010.

CLAWSON, K.L.; BLAD, B.L. Infrared thermometry for scheduling irrigation of corn. **Agronomy Journal**. v.74, p.311-316, 1982.

CLAWSON, K.L.; JACKSON, R.D.; PINTER, P.J. Evaluating plant water stress with canopy temperature differences. **Agronomy Journal.** v.81, p.858-863, 1989.

COHEN, Y.; ALCHANATIS, V.; SARANGA, Y.; ROSENBERG, O.; SELA, E.; BOSAK, A. Mapping Water Status Based on Aerial Thermal Imagery: Comparison of Methodologies for Upscaling from a Single Leaf to Commercial Fields. **Precision Agriculture**, v.18, p. 801-822, 2017. https://doi.org/10.1007/s11119-016-9484-3.

ĆOSIĆ, M. et al. Effects of irrigation regime and application of kaolin on canopy temperatures of sweet pepper and tomato. **Scientia Horticulturae**, v. 238, p. 23–31, 2018.

COSTA, J. M.; GRANT, O. M.; CHAVES, M. M. Thermography to explore plant–environment interactions. **Journal of Experimental Botany**, v. 64, n. 13, p. 3937–3949, 2013.

COSTA, J. O.; COELHO, R. D.; BARROS, T. H. S.; FRAGA JÚNIOR, E. F.; FERNANDES, A. L. T. Physiological responses of coffee tree under different irrigation levels. **Engenharia Agricola, Jaboticabal**, v. 38, n. 5, p. 648–656, 2018. DOI: https://doi.org/10.1590/1809-4430-Eng.Agric.v38n5p648-656/2018. Available at: https://www.scielo.br/j/eagri/a/y95V3fGcF4gNFg74qM7HBwQ/?format=pdf&lang=en.

COUVREUR, V.; KANDELOUS, M.M.; SANDEN, B.L.; LAMPINEN, B.D.; HOPMANS, J.W. Downscaling transpiration rate from field to tree scale. **Agricultural and Forest Meteorology, v.**221, p.71–77, 2016. doi:10.1016/j.agrformet.2016.02.008.

CONTRERAS, J. I.; ALONSO, F.; CÁNOVAS, G.; BAEZA, R. Irrigation management of greenhouse zucchini with different soil matric potential level. Agronomic and environmental effects. Agricultural Water Management, 183, p.26-34, 2017.

CRUSIOL, L. G.T; NANNI, M. R.; FURLANETTO, R. H.; SIBALDELLI, R. N. R.; CEZAR, E.; MERTZ-HENNING, L. M.; NEPOMUCENO, A. L; NEUMAIER, N.; FARIAS, J. R. B. UAV based thermal imaging in the assessment of water status of soybean plants, **International Journal of Remote Sensing**, 2019. DOI: 10.1080/01431161.2019.1673914

DEJONGE, K. C. et al. Comparison of canopy temperature-based water stress indices for maize. **Agricultural Water Management**, v. 156, p. 51–62, 2015. http://dx.doi.org/10.1016/j.agwat.2015.03.023

DING, Y.; ZHANG, Y.; ZHENG, Q.; TYREE, M. T. Pressure–volume curves: revisiting the impact of negative turgor during cell collapse by literature review and simulations of cell micromechanics. **New Phytologist**, v.203, p.378- 387, 2014.

DJEKOUN, A.; PLANCHON, C. Tolerance to low leaf water potential in soybean genotypes. **Euphytica**, v.55, p.247–253, 1991.

DOMINGUES, R.; PEREIRA, A.B.; SCHIEBELBEIN, L.M; BARBOSA, E. A. A. Beans cultivation and water regime on soil physical attributes. **Agricultural Engineering International**, No.3, v. 20, 2018.

EHSANI, R.; MAJA, J.M. The rise of small UAVs in precision agriculture. **Resour.Mag**, 20,18–19, 2013.

EKINZOG, E. K; SCHLERF, M; KRAFT, M; WERNER, F.; RIEDEL, A.; ROCK, G.; MALLICK, K. Revisiting crop water stress index based on potato field experiments in Northern Germany. **Agricultural Water Management**, 269, 107664, 2022.

ELSAYED, S. et al. Thermal imaging and passive reflectance sensing to estimate the water status and grain yield of wheat under different irrigation regimes. **Agricultural Water Management**, v. 189, p. 98–110, 2017.

ELSAYED, S.; MISTELE, B.; SCHMIDEHALTER, U. Can changes in leaf water potential be assessed spectrally? Funct. **Plant Biology,** v.38, p.523–533, 2011.

EMBRAPA. BRS FC104: Cultivar de Feijão-Comum Carioca Superprecoce. Comunicado Técnico. Santo Antonio de Góias, GO, Dezembro, 2017. ISSN 1678-961X

ERDEM, Y., ŞEHIRALI, S., ERDEM, T., KENAR, D. Determination of crop water stress index for irrigation scheduling of bean (*Phaseolus vulgaris* L.). **Turkish Journal of Agriculture and Forestry**, 30(3), 195–202, 2006.

FUCHS, M., TANNER, C.B. Infrared Thermometry of Vegetation1. **Agronomy Journal.** v.58, p.597-601, 1966. doi:10.2134/agronj1966.00021962005800060014x

FURLAN, D. A. Coeficiente de estresse hídrico utilizando termografia infravermelha - estudos em cafeeiro Conilon (*Coffea canephora*). Campos dos Goytacazes, RJ, 2017. 56 f. Dissertação (Mestrado em Produção Vegetal) - Universidade Estadual Norte Fluminense Darcy Ribeiro.

GALVÃO, Í. M.; DOS SANTOS, O. F.; DE SOUZA, M. L. C.; DE JESUS GUIMARÃES, J.; KÜHN, I. E.; BROETTO, F. Biostimulants action in common bean crop submitted to water deficit. **Agricultural Water Management**, Amsterdam, v. 225, n. August, p. 105762, 2019. Available at: https://www.sciencedirect.com/science/article/pii/S0378377419309746. DOI: https://doi.org/10.1016/j.agwat.2019.105762.

GARCÍA-TEJERO, I. F.; HERNÁNDEZ, A.; PADILLA-DÍAZ, C. M.; DIAZ-ESPEJO, A.; FERNÁNDEZ, J. E. Assessing plant water status in a hedgerow olive orchard from thermography at plant level. **Agricultural Water Management**, v. 188, p. 50–60, 2017.

GARDNER, W. R. Dynamic aspects of water availability to plants. **Soil Science**, v.89, p.63-73, 1960.

GARDNER, B.R., BLAD, B.L., GARRITY, D.P., WATTS, D.G. Relationships between crop temperature, grain yield, evapotranspiration and phenological development in two hybrids of moisture stressed sorghum. **Irrigation Science,** v.2, p.213-224, 1981a.

GARDNER, B.R., BLAD, B.L., WATTS, D.G. Plant and air temperatures in differentially irrigated corn. **Agricultural Meteorology**, v.25, p.207–217, 1981b.

GODYN, D.; HERBUR, E.; WALCZAK, J. Infraredthermography as a method for evaluating welfare of animals subjected to invasive procedures - a Review. **Annals of Animal Science**, v.13, p.423-434, 2013.

GONZÁLEZ-DUGO, V.; ZARCO-TEJADA, P.J.; NICOLÁS, E.; NORTES, P.A.; ALARCÓN, J.J.; INTRIGLIOLO, D. S.; FERERES, E. Using high resolution UAV thermal imagery to assess the variability in the water status of five fruit tree species within a commercial orchard. **Precision Agriculture**, v.14, p.660-678, 2013.

GONZALEZ-DUGO, V.; ZARCO-TEJADA, P. J.; INTRIGLIOLO, D. S; RAMÍREZ-CUESTA, J. Normalization of the crop water stress index to assess the within-field spatial variability of water stress sensitivity. **Precision Agriculture** 22: p.964–983, 2021. https://doi.org/10.1007/s11119-020-09768-6

HEYDARI, A; BIJANZADEH, E; R. NADERI, R; Y. EMAM, Y. Quantifying water stress in canola (Brassica napus L.) using crop water stress index**. Iran Agricultural Research** 38(1) 1-8, 2019.

HONRADO, J.L.E.; SOLPICO, D.B.; FAVILA, C.M.; TONGSON, E.; TANGONAN, G.L.; LIBATIQUE, N.J.C. UAV Imaging with low-cost multispectral imaging system for precision agriculture applications. In Proceedings of the 2017 IEEE Global Humanitarian Technology Conference (GHTC), San Jose, CA, USA, 19 October 2017.

IDSO, S. B. Non-water-stressed baselines: a key to measuring and interpreting plant water stress. **Agricultural Meteorology**, 27(1–2), 59–70, 1982.

IDSO, S. B.; JACKSON, R. D.; PINTER JÚNIOR, P. J.; REGINATO, R. J.; HATFIELD, J. L. Normalizing the stress-degree-day parameter for environmental variability. **Agricultural Meteorology**, v.24, p.45-55, 1981. https:// doi.org/10.1016/0002-1571(81)90032-7

IHUOMA, O.S; MADRAMOOTOO, C.A. Review: Recent advances in crop water stress detection. **Computers and Electronics in Agriculture**, v.141, p.267–275, 2017.

JACKSON R, D; REGINATO, R.J; IDSO, S.B. Wheat canopy temperature: a practical tool for evaluating water requirements. **Water Resources Research**, v.13, p.651-656, 1977.

JACKSON, R.D; IDSO, S.B; REGINATO, R.J; PINTER, P.J.J. Canopy temperature as a crop water stress indicator. **Water Resources Research**, v.17, p.1133-1138, 1981. https://doi.org/10.1029/ WR017i004p01133

JACKSON, R. D.; KUSTAS, W. P.; CHOUDHURY, B. J. A reexamination of the crop water stress index. **Irrigation Science**, v.9, p.309-317, 1988. https://doi.org/10.1007/BF00296705

JARVIS, P.G. The interpretation of the variations in leaf water potential and stomatal conductance found in canopies in the field. **Philosophical Transactions of the Royal Society B: Biological Sciences**., v.273, p.593-610, 1976.

JIANG, J.; HUO, Z.; FENG, S.; KANG, S.; WANG, F.; ZHANG, C. Effects of deficit irrigation with saline water on spring wheat growth and yield in arid Northwest China. **Journal of Arid Land**, v.5, p.43–154, 2013.

JIMÉNEZ-BELLO, M.A., BALLESTER, C., CASTEL, J.R., INTRIGLIOLO, D.S. Development and validation of an automatic thermal imaging process for assessing plant water status. **Agric. Water Manag**. V.98, p.1497-1504, 2011. doi:10.1016/j.agwat.2011.05.002

KETELLAPER, H. J. Stomatal physiology. **Ann. Rev. Plant Physiol**. v.14. p.249-70, 1963.
KHANAL, S.; FULTON, J.; SHEARER, S. Review An overview of current and potential applications of thermal remote sensing in precision agriculture. **Computers and Electronics in Agriculture**, v.139, p.22–32, 2017.

KHATAR, M.; MOHAMMADI, M.H; SHEKARI, F. Some physiological responses of wheat and bean to soil salinity at low matric suctions. **International Agrophysics**, v.31, p.83-91, 2017. doi: 10.1515/intag-2016-0028

KHORSAND, A. et al. Irrigation scheduling of maize based on plant and soil indices with surface drip irrigation subjected to diferent irrigation regimes. **Agric. Water Manag**. 224, 105740. https://doi.org/10.1016/j.agwat.2019.105740 (2019).

KIRNAK, H; IRIK, H.A; UNLUKARA, A. Potential use of crop water stress index (CWSI) in irrigation scheduling of drip-irrigated seed pumpkin plants with different irrigation levels. **Scientia Horticulturae**. Volume 256, 2019. https://doi.org/10.1016/j.scienta.2019.108608

LEINONEN, I.; JONES, H.G. Combining thermal and visible imagery for estimating canopy temperature and identifying plant stress. **J. Exp. Bot**. v.55, p.1423–1431, 2004.

LIPAN, L.; ISSA-ISSA, H.; MORIANA, A.; ZURITA, N.M.; GALINDO, A.; MARTÍN-PALOMO, M.J.; ANDREU, L.; CARBONELL-BARRACHINA, Á.A.; HERNÁNDEZ, F.; CORELL, M. Scheduling Regulated Deficit Irrigation with Leaf Water Potential of Cherry Tomato in Greenhouse and its Effect on Fruit Quality. **Agriculture** 2021, 11, 669. https://doi.org/10.3390/ agriculture11070669

MAES, W. H.; STEPPE, K. Estimating evapotranspiration and drought stress with ground-based thermal remote sensing in agriculture: a review. **Journal of Experimental Botany**, v.63, p.4671-4712, 2012.

MARSHALL, T. J. Relations between water and soil. Tech. Commun. No. 50. Harpenden, U.K.: Commonwealth Bureau Soils. 1959.

MATHOBO, R., MARAIS, D., STEYN, J. The effect of drought stress on yield, leaf gaseous exchange and chlorophyll fluorescence of dry beans (Stageolus vulgaris L.). **Agric. Water Manag**. 180, 118–125. 2017. https://doi.org/10.1016/j.agwat.2016.11.005.

NASCIMENTO, D. A.; BRITO, A.S.; SILVA, L. M.N.; PEIXOUTO, S. L.; COTRIM, V.F. Water use efficiency of castor bean under semi-arid conditions of Brazil. **Agricultural Water Management** 260, 2022. Https://doi.org/10.1016/j.agwat.2021.107278

NOURI, S; NASROLAHI, A; MALEKI, A.; SHARIFIPOUR, M. Estimation of soil moisture content using Crop Water Stress Index for Irrigation management of Pinto bean. **Iranian Journal of Irrigation and Drainage**. No.1, vol.14, Apr-May, p.136-145. 2020.

O'SHAUGHNESSY, S. A. et al. A crop water stress index and time threshold for automatic irrigation scheduling of grain sorghum. **Agricultural Water Management**, v. 107, p. 122-132, maio 2012.

O'SHAUGHNESSY, S. A., EVETT, S. R., COLIAZZI, P. D., & HOWELL, T. A. Soil water measurement and thermal indices for center pivot irrigation scheduling. Irrigation Association Conference Proceedings Anaheim, California, 23-33, 2008.

PACHECO, F.B.P.; REICHARDT; K.; TUON, R.L. Variabilidade espacial e temporal do potencial mátrico da água em terra roxa estruturada. **Sci. agric**., Piracicaba, 51 (2): 327-334, maio/ago., 1994.

PADHI, J.; MISRA, R. K.; PAYERO, J. O. Estimation of Soil Water Deficit In An Irrigated Cotton Field With Infrared Thermography. **Field Crops Research**, v.126, p.45-55, 2012.

PARK, S., RYU, D., FUENTES, S., CHUNG, H., HERNÁNDEZ-MONTES, E., & O'CONNELL, M. Adaptive estimation of crop water stress in nectarine and peach orchards using high-resolution imagery from an unmanned aerial vehicle (UAV). **Remote Sensing**, 9(8), 828, 2017.

PARK, S.; RYU, D.; FUENTES, S.; CHUNG, H.; O'CONNELL, M.; KIM, J. Dependence of CWSI-Based Plant Water Stress Estimation with Diurnal Acquisition Times in a Nectarine Orchard. **Remote Sensing**. 2021, 13, 2775. https://doi.org/10.3390/rs13142775

PLAŠČAK, I; JURIŠIĆ, M.; RADOČAJ, D.; VUJIĆ, M.; ZIMMER, D. An Overview of Precision Irrigation Systems Used in Agriculture**. Technical Journ**AL 15, p.546-553, 2021. https://doi.org/10.31803/tg-20210416103500

PEREIRA, R. M. Manejo de irrigação com automação de baixo custo no cultivo da alface submetida a diferentes potenciais matriciais do solo 118 p.: il. Tese (Doutorado em Agronomia) – Universidade de Brasília / Faculdade de Agronomia e Medicina Veterinária, 2021.

PETERS, R. T.; EVETT, S. R. Complete center pivot automation using the temperature-time threshold method of irrigation scheduling. 2004 ASAE/CSAE Annual International Meeting, Ottowa, Ontario, Canada, 042196, 2004.

POSSIGNOLO, ISABELLA PRESOTTO, "Using Infrared Radiometry Thermometer for Irrigation Management of Dry Edible Beans in Western Nebraska" (2020). Biological Systems Engineering--Dissertations, Theses, and Student Research. 104.
https://digitalcommons.unl.edu/biosysengdiss/104

PRADAWET, C.; KHONGDEE, N.; HILGER, T.; CADISCH, G. Thermal imaging for assessment of maize water stress and yield prediction under drought conditions. **Journal of Agronomy and Crop Science**, p. 1-15, 2022. DOI: 10.1111/jac.12582

QUILOANGO-CHIMARRO, C.; COELHO, R. D.; COSTA, J. de O.; GOMEZ-ARRIETA, R. CROP WATER STRESS INDEX FOR PREDICTING YIELD LOSS IN COMMON BEAN. **IRRIGA**, *[S. l.]*, v. 1, n. 4, p. 687–695, 2021. DOI: 10.15809/irriga.2021v1n4p687-695. Available on: https://revistas.fca.unesp.br/index.php/irriga/article/view/4425. Access on: mar. 25th,2022.

RAMÍREZ, A. J. F.; COELHO, R. D.; PIZANI, M. A. M.; SILVA, C. J. da. Determinação do índice de estresse hídrico em tomateiros cereja (*Lycopersicum Solanum* var. Cerasiforme.) com câmara infravermelha. **Revista Brasileira de Agricultura Irrigada**, v.9, p.218-224, 2015. https://doi.org/10.7127/rbai.v9n400356

ROMANO, G.; ZIA, S.; SPREER, W.; SANCHEZ, C.; CAIRNS, J; ARAUS, J.L.; MÜLLER, J. Use of thermography for high throughput phenotyping of tropical maize adaptation in water stress. **Computers and Electronics in Agriculture**, v. 79, p. 67-74, 2011.

SCHOLANDER, P. F.; HAMMEL, H. T.; HEMINGSEN, E. A.; BRADSTREET, E. D. Hydrostatic pressure and osmotic potencials in leaves of mangroves and some other plants. **Proceedings of National Academy Science**, v.51, p.119-125, 1964.

SCHOLANDER, P. F.; HAMMEL, H. T.; BRADSTREET, E. D.; HEMMINGSEN, E. A. Sap pressure in vascular plants. **Science**, v.148, p.339 -446, 1965.

SHELLIE, K.C; KING, B. A. Application of a Daily Crop Water Stress Index to Deficit Irrigate Malbec Grapevine under Semi-Arid Conditions. **Agriculture**, 10, 492, 2020. doi:10.3390/agriculture10110492

SIKKA, A. Automated irrigation system using IOT. **International Research Journal of Engineering and Technology (IRJET)** 5(3), p.1831-1834, 2018.

SILVA, C. J.; SILVA, C. A.; FREITAS, C. A.; GOLYNSKI, A.; SILVA, L. F. M.; FRIZZONE, J. A. Tomato water stress index as a function of irrigation depths. **Revista Brasileira de Engenharia Agrícola e Ambiental Campina Grande**, PB, UAEA/UFCG. v.22, n.2, p.95-100, 2018. DOI: http://dx.doi.org/10.1590/1807-1929/agriambi.v22n2p95-100

SILVA, A. V.; SILVA FILHO, J. F.; SILVA, M. C. T.; VAZ, N. C. A.; SILVA, M. L. G. Aptidão edafoclimática e ambientes de produção agrícola da cultura do feijão. **Scientific Electronic Archives**, Vol. 13 (10), 2020. http://dx.doi.org/10.36560/131020201114

SISHODIA, R. P.; RAY, R, L.; SINGH, S. K. Applications of Remote Sensing in Precision Agriculture: A Review. **Remote Sens**, 12, 3136, 2020. doi:10.3390/rs12193136

SLATYER, R. O. Plant-Water Relationships. **Academic Press**, New York. p.366, 1967.

SMART, D.R.; TARYN, L.; BAUERLE, C.S; EISSENSTAT, D, M. Root survivorship under deficit and dryland farming conditions for 1103P and 101-14MGT rootstocks in the Oakville region of the Napa Valley. 7th **International Symposium on Grapevine Physiology and Biotechnology**, June 21–25, 2004, University of California, Davis, CA. 2004.

SOUSA, D. M. G. de; LOBATO, E. (ed). **Cerrado: correção do solo e adubação**. 2. ed. Brasília, DF: Embrapa Informação Tecnológica; Planaltina, DF: Embrapa Cerrados, 2004. P.416 p. il.

TANNER, C. B. Plant temperatures. **Agronomy Journal**. v.55, p.210-211, 1963. https://doi.org/10.2134/agronj1963.00021962005500020043x

TAGHVAEIAN, S., CHAVEZ, J.L., BAUSCH, W.C., DEJONGE, K.C., TROUT, T.J. Minimizing instrumentation requirement for estimating crop water stress index and transpiration of maize. **Irrig. Sci**. 32 (1), p.53–65, 2014.

TAIZ, L.; ZEIGER, E. **Plant physiology** (sixth edition). Universitat Jaume I, 2015.
UPCHURCH, D. R.; WANJURA, D.F.; BURKE, J.J.; MAHAN, F.R. Biologically-identified Optimal Temperature Interactice Console (Biotic) for Managing Irrigation, U.S. Patent., 1996.

VIEIRA, G.H.S.; FERRAREZI, R.S. Use of Thermal Imaging to Assess Water Status in Citrus Plants in Greenhouses. **Horticulturae**, 7, 249, 2021. https://doi.org/10.3390/ horticulturae7080249

XU, J., Y. LV, X. LIU, T. DALSON, S. YANG AND J. WU. Diagnosing crop water stress of rice using infra-red thermal imager under water deficit condition. **Int. J. Agric. Biol**., 18: 565–572.2016. DOI: 10.17957/IJAB/15.0125

WIJEWARDANAA, C; ALSAJRIA, F. A.; IRBYA, J. T.; KRUTZ, L. J.; GOLDENC, B.; HENRYA, W. B.; GAOD, W.; REDDYA, K. R. Physiological assessment of water deficit in soybean using midday leaf water potential and spectral features. **Journal of plant interactions**, VOL. 14, NO. 1, p.533–543, 2019. https://doi.org/10.1080/17429145.2019.1662499

ZARCO-TEJADA, P. J.; GONZÁLEZ-DUGO, V.; BERNI, J. A. J. FLUORESCENCE. Temperature And Narrow-Band Indices Acquired from A UAV Platform For Water Stress Detection Using A Micro-Hyperspectral Imager And A Thermal Camera. **Remote Sensing of Environment**, v.117, p.322-337, 2012.

ZHUANG, S.; WANG, P.; JIANG, B.; LI, M.; GONG, Z. Early detection of water stress in maize based on digital images. **Comput. Electron. Agric**. 140, 461–468, 2017.